CHALMERS

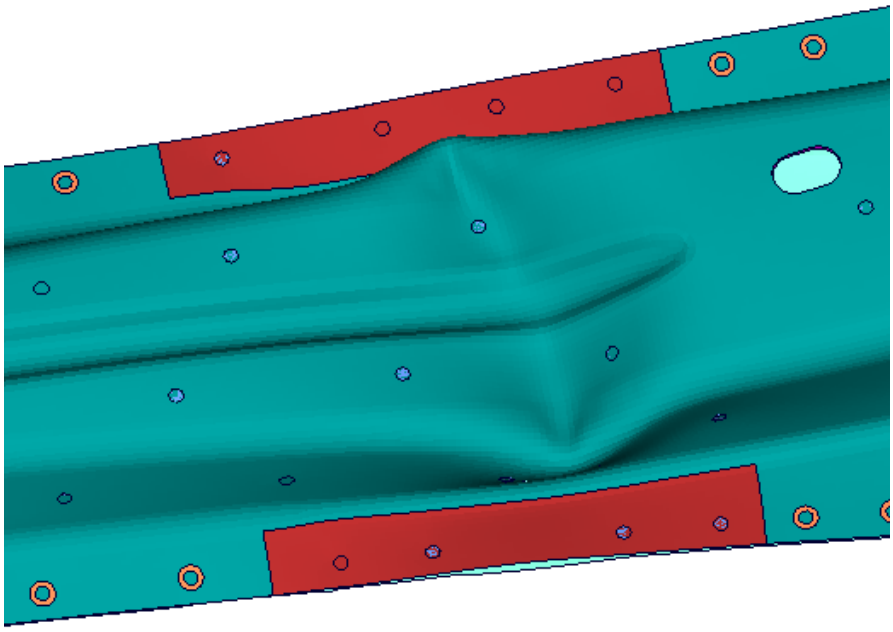

Tempering of hot-formed steel using induction heating

Master of Science Thesis

OLOF HEDEGÄRD
MARTIN ÅSLUND

Department of Materials and Manufacturing Technology
CHALMERS UNIVERSITY OF TECHNOLOGY
Gothenburg, Sweden, 2011
Report No. 54/2011

Tempering of hot-formed steel using induction heating

by

OLOF P. HEDEGÄRD
MARTIN A. T. ÅSLUND

Diploma work No. 54/2011

at Department of Materials and Manufacturing Technology

CHALMERS UNIVERSITY OF TECHNOLOGY

Gothenburg, Sweden

Diploma work in the Master programme Product Development

Performed at:	Body Structure Engineering, Volvo Car Corporation, SE – 405 31 Gothenburg
Supervisors:	Mikael Fermér, Richard Johansson & Peter Nyström Body Structure Engineering, Volvo Car Corporation, SE – 405 31 Gothenburg
Examiner:	Docent Johan Ahlström Department of Materials and Manufacturing Technology Chalmers University of Technology, SE - 412 96 Gothenburg

Tempering of hot-formed steel using induction heating

OLOF P. HEDEGÄRD
MARTIN A. T. ÅSLUND

Diploma work no 54/2011
Department of Materials and Manufacturing Technology
Chalmers University of Technology
SE-412 96 Gothenburg
Sweden
Telephone + 46 (0)31-772 1000

Cover:
CAE simulation of a B-pillar with tempered flanges exposed to 3-point drop tower test.

Chalmers Reproservice
Gothenburg, Sweden 2011

Tempering of hot-formed steel using induction heating

OLOF P. HEDEGÄRD
MARTIN A. T. ÅSLUND
Department of Materials and Manufacturing Technology
Chalmers University of Technology

Abstract

Hot-formed martensitic boron steel plate offers very high strength and is therefore useful in car bodies in areas where deformation should be kept to a minimum, like the safety cage. However, cracks may initiate around spot welds during mechanical loading. The problem mainly originates from the lower yield strength in the heat-affected zones (HAZ) as compared to the surrounding structure, causing strain localization. In this project the possibility to prevent cracking by induction tempering before spot welding has been investigated. The idea has been to distribute strains and avoid localization around welds. Tensile tests have been performed on samples tempered in furnace and by induction heating, with and without spot welds. The results show that the weakening effect from the spot weld can be eliminated by a tempering operation. Further, high strain rate 3-point drop tower tests have been performed on full scale B-pillars with and without tempered flanges. B-pillars with tempered flanges show promising results compared to fully hardened. According to the results additional kinetic energy absorption of 30% at crack initiation was observed.

Keywords: Boron steel, HAZ, Tempering of martensite, Induction tempering.

Preface

This master thesis was carried out during the spring 2011 at Body Structure Engineering at Volvo Car Corporation by two students with background from mechanical engineering. It is the final part of the master program Product Development at Chalmers University of Technology. The project has been very educative, where we have really broadened our view within this field of engineering.

We would like to thank our supervisors Mikael Fermér, Richard Johansson and Peter Nyström at Volvo Car Corporation for their technical expertise and commitment and our examiner Johan Ahlström, Department of Materials and Manufacturing Technology for support and guidance.

We would also like to thank everyone from different departments at Volvo for helping us during the project with technical matters.

Gothenburg, June 2011

Olof Hedegärd
Martin Åslund

Table of Contents

1 Introduction

1.1 Background

There is currently a strong focus in the automotive industry to reduce the environmental impact, where one way is to lower the weight of the car to minimize fuel and material consumption. Boron steel, also known as hot-formed steel or ultra high strength steel (UHSS), offers the possibility to reduce the weight while retaining or enhancing the crash performance. It offers extreme strength, good formability and minimal spring back at a relatively low cost. The disadvantages are the low ductility and high sensitivity to geometrical and metallurgical notches, such as holes and spot welds. Hot-formed parts are especially useful in areas where the deformation should be kept to a minimum, such as the car body safety cage.

1.2 Goal

The goal is to investigate and analyze the effects of short time tempering of boron steel using induction heating. It is desired to locally reduce the strength and increase the ductility within a hot-formed boron steel part, to minimize risk of crack initiation and enhance the total structural strength.

1.3 Problem description

Welding creates very soft and weak heat affected zones (HAZ) in martensitic steels (1). These zones tend to fail at relatively low stresses, reducing the total strength of structures. This problem mainly originates from the difference in material strength within the spot weld and the surrounding martensitic region. Due to this difference in material properties, the deformation tends to be localized to the weaker HAZ, which results in early crack initiation.

It is desired to prevent cracking, i.e. eliminate this localized deformation while retaining other critical properties such as strength and ductility of the material, at a sufficient level. It may be realized by creating a larger surrounding zone which is softer and can distribute the deformation, hence preventing a localized deformation and the early crack initiation.

There is currently a great interest for developing methods and tools to locally soften boron steel parts. This technique also has several other potential areas, since tailoring material properties within a part may be very beneficial. One reason is the advantages of modifying a part to possess certain material properties within specific areas, maximizing the structural functionalities.

Local softening can be accomplished in different ways, where one route is to temper an already hot-formed martensitic part in a second operation. This method has several benefits since size, position and number of "soft zones" can be determined very late in the projects.

Regular methods for tempering components are usually time consuming with tempering time up to hours (2), not suitable for production in the automotive industry. Therefore, short-time tempering is of great interest and has been investigated and analyzed in this project.

1.4 Methodology

A literature study was done early in the project to increase knowledge in the specific area of material science (boron steels, tempering, microstructures etc). Databases accessible through Chalmers library, books and expertise from Chalmers and Volvo Car Corporation (VCC) were used as resources. The essential theory for the project is summarized in the report. All information used throughout the project was carefully compiled from the literature and resource base and then thoroughly discussed and analyzed before proceeding. Technical experts were consulted when important decisions had to be made.

Tempering is a heat treatment where the material is exposed to elevated temperature for a specific period of time and then slowly cooled to room temperature. This will cause changes in the microstructure of the material and its properties such as ductility, strength and hardness.

Tempering was first realized in the interval 500°C-700°C at test specimens of the boron steel, using a *furnace*, see Figure 1 (a). 11 specimens were treated at respective temperature (500°C, 600°C and 700°C) whereof five specimens were spot welded afterwards. Tensile tests, hardness tests and metallurgical analysis were carried out to investigate changes in material behavior after the different tempering treatments, see Figure 1 (c-e).

This process was then repeated at the same type of specimens using *induction heating* in the interval 400°C-600°C. Identical tests were performed to get a comparison between tempering effects of the two heating processes.

Based on the results from these experimental series, an appropriate procedure for tempering of B-pillars was designed. The B-pillars were tempered along the flanges to achieve soft zones, see Figure 2(a-b).

An important function of the B-pillar is to enhance crash performance and secure safety for passengers during side impacts. The cracks may initiate in the HAZ in the flanges during deformation/impact and then grow into the beam structure, reducing the strength substantially. The B-pillars were tested in a 3-point drop tower test at VCC after an initial CAE study done at Volvo Cars for estimating the behavior, see Figure 2 (c-d).

The results from the three experimental series were analyzed, discussed and concluded. Recommendations for further research and development were written.

1.5 Delimitations

The study shall contain the following delimitations:

- No other material than 22MnB5 will be considered.
- No CAE-simulation or calculations will be developed, only used to increase knowledge concerning structural strength of a B-pillar.
- Tensile test and 3-point drop tower test will only be performed at room temperature.
- The study will not include an optimization of tempering temperature.
- The study will not include an optimization of tempered area on B-pillars.

- No exhaustive analysis concerning desired, optimal material properties of B-pillar will be developed
- The study will run no more than 20 weeks.
- All tests will be done according to routines commonly used at VCC.
- No industrial implementation or process will be developed.
- No geometrical measurement or analysis will be compiled.

Tempering of specimens

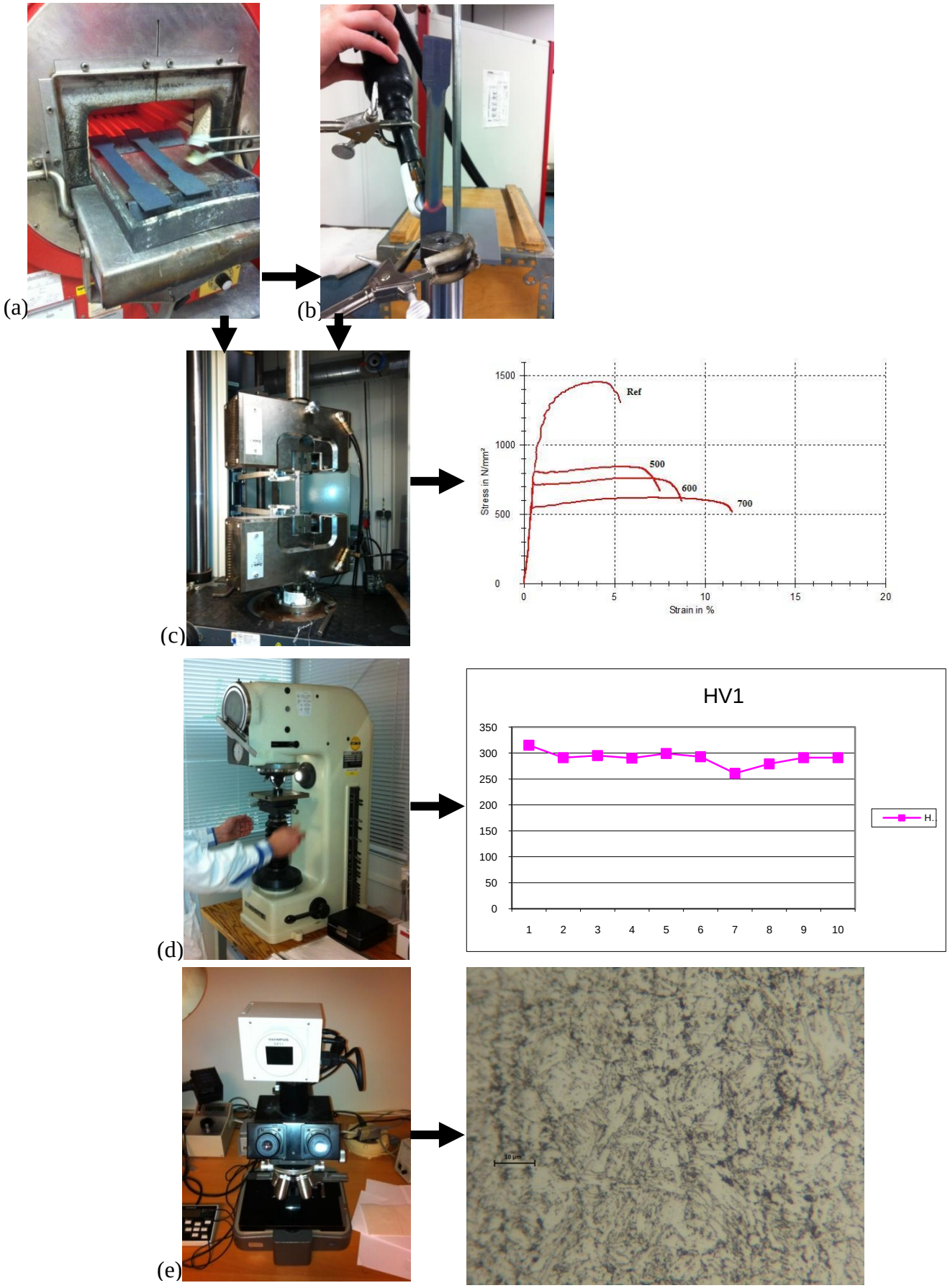

Figure 1: Tempering of simple specimen using (a) furnace heating, (b) induction heating. Specimens were later exposed to (c) tensile tests (d) hardness tests (e) microstructure analysis.

Tempering of B-pillars

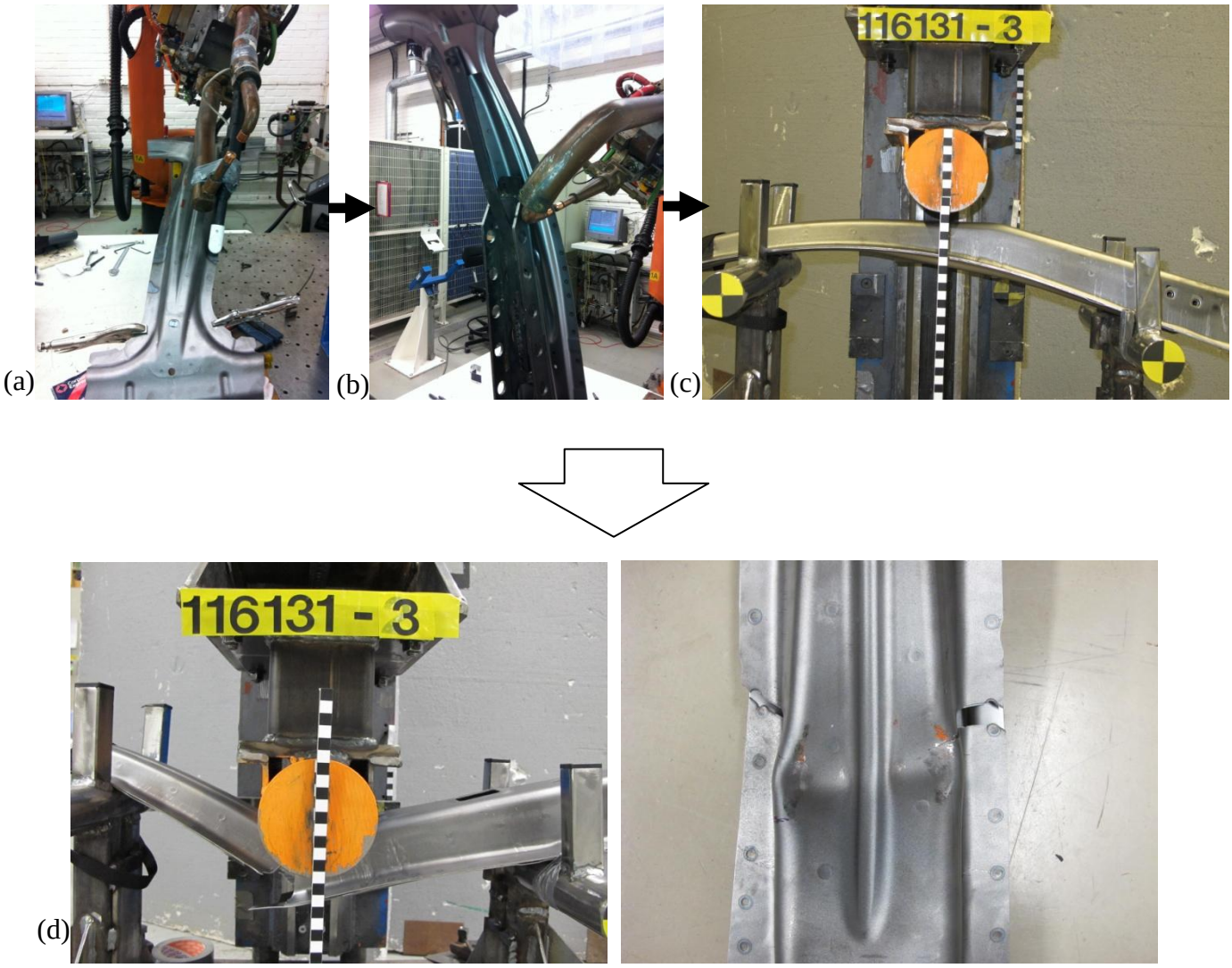

Figure 2: (a) induction tempering of flanges of B-pillars, using an industrial robot. (b) Tempered and fully hardened B-pillars were spot welded along the flanges. (c) 20 B-pillars were tested in a 3-point drop tower test at different velocities. (d) Comparison between tempered and fully hardened B-pillars.

2 Theory

This chapter contains the basic theory relevant for the study. The purpose is to give a theoretical base of the subject in order to understand the experimental process and results.

2.1 Hot stamped boron steel 22MnB5

The boron-alloyed steel 22MnB5 has a ferritic-pearlitic microstructure after normalization. However, in applications it is often used in hardened state, formed in a hot-stamping process where forming and hardening are done in the same operation. Blanks are austenitized at temperatures around 950°C in a furnace and subsequently transferred for stamping in a cooled die. In the die, the material is often quenched to a completely martensitic structure. To assure a completely martensitic structure the cooling temperature must be at least 30°C/s (3). This material is more prone to form martensite compared to plain carbon steel. At the high temperatures the material has very good formability and is easily formed into complex shapes. After austenitization and quenching the part has a minimum ultimate tensile strength of 1300 MPa and minimum yield strength of 950 MPa. The material will be almost free from internal stresses and show little spring back. The composition of the material is given in Table 1.

Table 1: Composition of boron steel 22MnB5 (4)

C [%]	Si [%]	Mn [%]	P [%]	S [%]	Cr [%]	Mo [%]	B [%]	Ti [%]	A [%]
0.2-0.25	0.15-0.5	1.00-1.40	0.03 max	0.025 max	0.1-0.35	0.35 max	0.0015-0.0050	0.03-0.05	0.02-0.06

If the boron steel is uncoated an iron oxide layer will form on the surface as the blank is transported from the furnace to the die. This would require second descaling operation using sand blasting or pickling. This can be avoided by an Al-Si coating of the surface. During the heat treatment and quenching the Al-Si layer is transformed into a protective Fe-Al-Si alloy layer. The surface layer protects the steel from oxidation and decarburization, but do not have the function as a cathodic corrosion protection. In this project the Al-Si-coated 22MnB5 steel with the trade name Usibor 1500 has been used for all test specimens except for the B-pillars that were made from uncoated boron steel.

2.2 HAZ (Heat Affected Zone) in spot welded pearlitic steels

Spot welding is the most common welding processes for joining automotive parts. The heat-affected zone (HAZ) is the area around the fusion zone (weld) that has its microstructure and properties changed during welding. Any portion that is heated above certain temperature levels will be affected regarding microstructure and properties after cooling.

Due to the temperature gradient, the heat affected zone consists of different structures in different regions, see Figure 3.

Subcritical region (480-730°C)

The material around the fusion zone may be affected by a short time tempering treatment, see Figure 3. In this region Fe_3C carbides start to cluster and create a fine dispersion of small carbide particles embedded within a continuous α-iron matrix that result in reduced strength and hardness together with increased ductility (5).

Intercritical region (730°C – Austenite)

In the intercritical region there is a partial transformation to austenite. The austenite can later transform to ferrite, pearlite or to martensite upon cooling. This transformation is dependent on cooling rate and composition (6).

Supercritical region (Austenite region)

In the supercritical region there is a complete transformation to austenite, which transforms to ferrite, pearlite, martensite or martensite with residual austenite upon cooling depending on cooling rate and composition. The volumes of the HAZ that exceeds ca 1050°C will experience grain growth. Grain growth results in decrease of toughness in the coarse-grain-region. The higher the temperature, and the longer the time, the more grain growth will occur. (7).

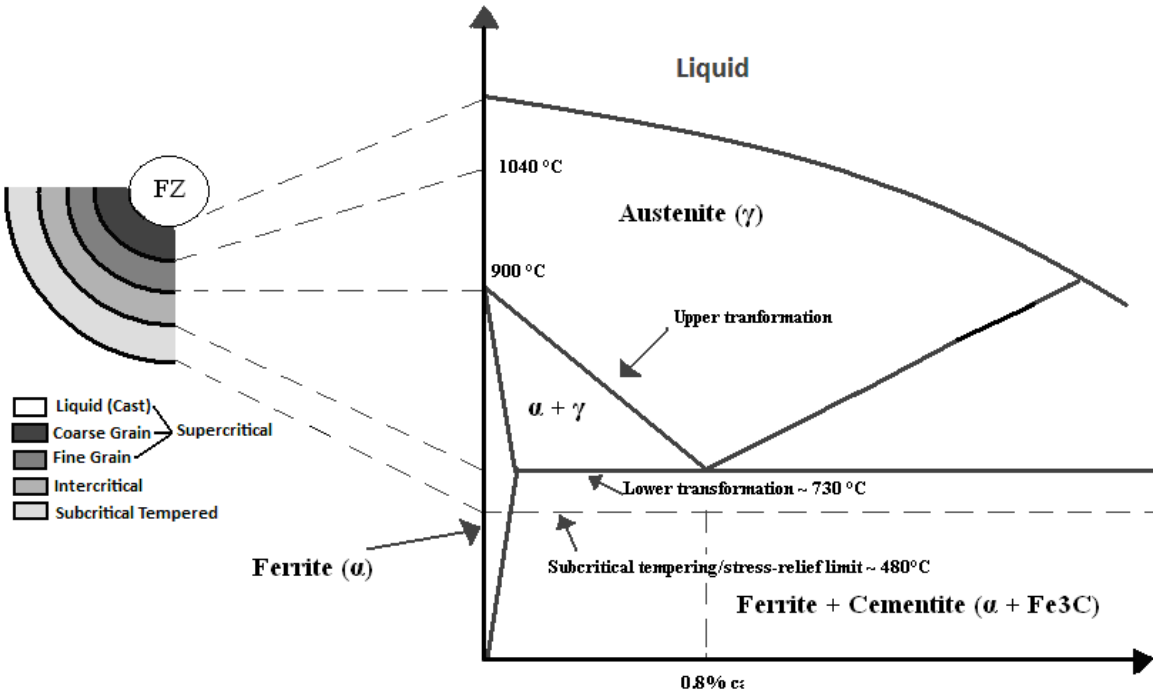

Figure 3: Phase diagram for steels with marked areas of the heat affected zone around a spot weld. Reproduced by Martin Åslund (7)

2.3 HAZ (Heat Affected Zone) in spot welded martenstic boron steel

After hot forming, the martensitic boron steel has a hardness of approximately 500 HV1 (8). When welded, the martensite becomes tempered in the heat-affected zone resulting in hardness just over 300 HV1. The weld is melted and then quenched, resulting in a re-created martensitic structure of the same hardness as the base material (500 HV1). The surrounding material as well as the weld itself thus have similar hardness, see Figure 4.

Some of the material properties will deteriorate after a thermal welding cycle i.e. the martensitic steel will decrease in both strength and ductility. This degradation of material properties, after welding, is attributed to the creation of local soft zones in the region. The small heat affected zone where the material is softer makes it recipient to strain during loads. As the strain is concentrated to this volume, crack initiation and propagation starts earlier.Some partial embrittlement may also occur in the coarse-grain-zone close to the weld in the HAZ (5). These two major effects are the primary reasons for decrease in fracture toughness of the material; soft zones acts as localized areas for the deformation while the coarse-grained-zone is brittle with poor ductility.

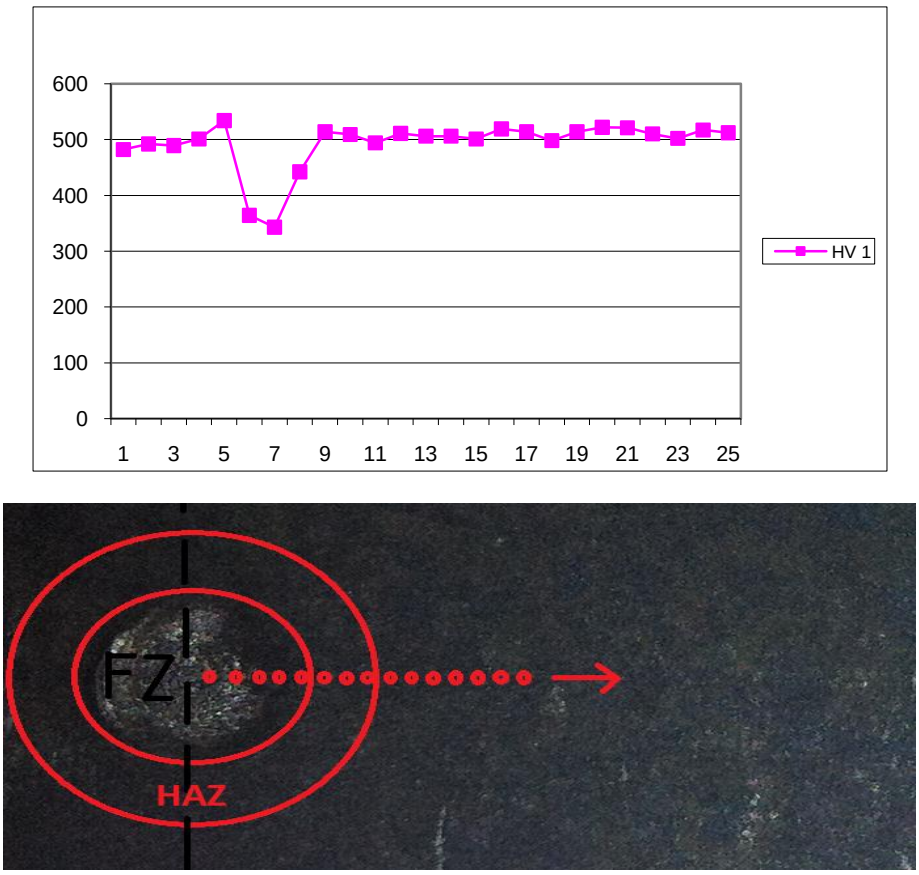

Figure 4: Hardness around spot weld in martensitic 22MnB5 over the cross section of a test specimen with a weld applied in the middle.

2.4 Tempering of martensite

In the as-quenched state, martensite is very hard and therefore a very useful material in specific areas due to its hardness and high tensile – and yield strength. It is also a brittle material which for many applications requires heat treatment to increase ductility at the expense of material strength. Such a heat treatment is known as *tempering*, making it more resistant to brittle fracture (5).

Tempering is realized by heating martensitic steel to a certain temperature level below the eutectoid temperature (~730°C) for a specific period of time, making the steel more ductile while reducing hardness and strength.

Tempering results in changes in the microstructure and mechanical properties as the meta stable martensitic structure is held isothermally at a temperature where austenite cannot form. It is a process in which the material structure deviates from quenched martensite under the influence of thermal activation (9). Normally, tempering is carried out at temperatures between 250-650 °C, though this is dependent on alloying constituents and time (5).

Tempering heat treatment allows, by diffusion processes, the formation of tempered martensite, according to the reaction:

Martensite (BCT, single phase) ➔ Tempered martensite ($\alpha + Fe_3C$ phase)

Basically, untempered martensite is a supersaturated solid state of carbon in iron which, during tempering, rejects the carbon. All the carbon atoms are positioned as interstitial impurities in the as-quenched martensite, and are therefore capable of rapidly transforming into other structures if heated to temperatures at which diffusion rates become active. The structure then gradually transforms to a mixture of regular body centered cubic (BCC) ferrite and cementite Fe_3C (1).

A moderately tempered martensite is a very fine dispersion of small carbide particles embedded within a continuous ferrite matrix. This new combination of phases is a more ductile material with increased toughness and it often has little similarity with the original as-quenched martensite (10). These changes in material properties might be explained by the large ferrite-cementite boundary area per unit volume for the very fine structure; impeding dislocation motion. The hard cementite also reinforces the soft ferrite matrix along boundaries, making it relatively strong and hard, but more ductile and tough due to the continuous ferrite matrix. The size of the cementite particles influences the mechanical behavior of the material. Small size maximizes the ferrite-cementite boundary areas, resulting in stronger but less ductile material, and vice-versa.

Furthermore, the heat treatment determines the size of the cementite particles, i.e. the variables temperature and time influences the final structure and mechanical properties.

Since carbon diffusion is highly dependent on temperature, increasing the heat treatment temperature will accelerate diffusion, the rate of cementite particles growth and softening of the steel (5).

Table 2: Tempering reactions at different temperatures (11).

Temperature (°C)	Transformation
350-550	Segregation of impurities and alloying elements
400-600	Recovery of dislocation substructure. Cementite (Fe_3C) creates cluster spheroidal carbides
600-700	Recrystallisation and grain growth; coarsening of spheroidal cementite (Fe_3C)

2.5 Short time tempering

Tempering is usually accomplished through isothermal heating under a sufficient period of time. Though, some studies have been made investigating short time tempering effect on microstructure and mechanical properties of martensitic steels. It has been found that martensitic steel shows a very rapid softening upon tempering. During the first 0.1 seconds the hardness decrease has been measured up to 35-55% for tempering temperatures 500-700°C. In contrast, additional hardness decrease was only ~10-15% of the original hardness, even after 30 minutes (12). The study also shows that the maximum temperature has a major influence on the tempering effect compared to time.

3 Experimental process

This study is to a large extent based on tests and experiments that are explained below. The experimental process was launched after an initial literature study.

3.1 Test specimens

Test specimens were laser cut from a metal sheet to form a simple, flat, standard test specimen with appropriate length according to the European standard for tensile testing (A8 or A80), where the total elongation is measured(13). For a complete geometry description see Figure 5. The specimens were laser cut in the rolled direction of the sheet to assure consistent values throughout the project. The experimental series are summarized in Table 3.

Table 3: Number of specimens used in the experimental series.

Treatment	#
Reference	11
Furnace tempered 500°C	11
Furnace tempered 600°C	11
Furnace tempered 700°C	11
Induction tempered 400°C	10
Induction tempered 500°C	10
Induction tempered 600°C	10

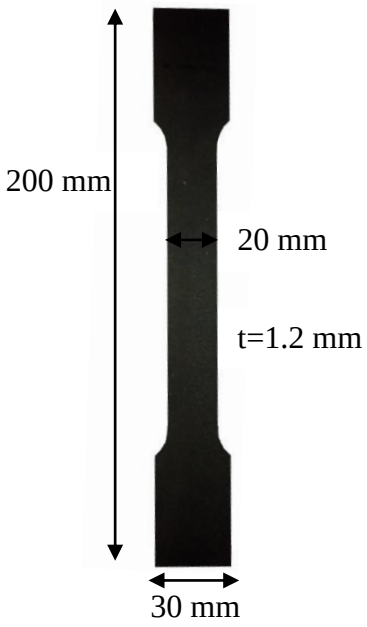

Figure 5: Dimensions of the test specimens used in the experimental series.

3.2 Furnace tempering

Furnace tempering was carried out at the department for Surface Treatment at VCC. It was realized in a muffle furnace of the model Heraeus MR 170E with a maximum temperature of 1100°C. To verify the temperature achieved in the furnace, an external thermometer was used.

The specimens were placed over two small supporting beams to avoid contact with the furnace. Due to the small size of the furnace, the specimens were heated in batches of four or less. Tempering was carried out for five minutes at 500°C, 600°C and 700°C respectively. The temperatures were chosen to map the tempering effects within this interval.

After heat treatment, ten specimens were tensile tested and one was hardness tested, for respective temperature. On five of the specimens a single spot weld was placed in the middle before tensile testing. The stress-strain behavior is of great interest when investigating the ductility and strength of the material. The tempered specimens were tested in a universal testing machine at VCC, equipped with an extensometer to measure the elongation. Due to

insufficient maximum load capacity of the grips, the fully hardened specimens with a tensile strength exceeding 30 kN were instead tested at IUC (Industriellt UtvecklingsCentrum) in Olofström. Also a number of specimens tempered at 700°C were tested at IUC for comparison of the results. The tests resulted in tensile test curves where e.g. tensile strength, yield strength and elongation could be deduced. All the tests were performed with a constant tensile speed of 10 mm/min. The tensile tests at IUC were monitored with ARAMIS, a three-dimensional video system to analyze the strain and deformation during loading (14).

The last specimen was used for hardness test and microstructure analysis. Hardness tests were carried out at VCC to investigate the influence from the different tempering processes. The hardness was measured with a Vickers indentor (8) with a load of 1 kg (HV1). Optical microscopy was performed at Chalmers to investigate the microstructure of the tempered specimens. Pictures were taken at approximately 320x and 1000x magnification. To prepare for this operation, the specimens had to be polished and etched. The etching was made with Nital.

Further specimens were tempered in the same furnace to investigate volume changes for each temperature. The length of the specimens was measured before and after the tempering.

3.3 Induction tempering

Induction heating is a process where electromagnetic induction is used to heat an electrically conducting material. An AC current going through an induction coil generates an alternating magnetic field. When the part to be heated is placed within the magnetic field, eddy currents are induced in the material. Heat is produced in the material where the eddy currents flow due to its resistivity.

An automated linear movement was used to get an even distribution of the heat during the tempering process. This was performed with a tensile test machine at VCC, where the specimen was attached to the machine and moved along the induction heater with specified velocity, see Figure 6.

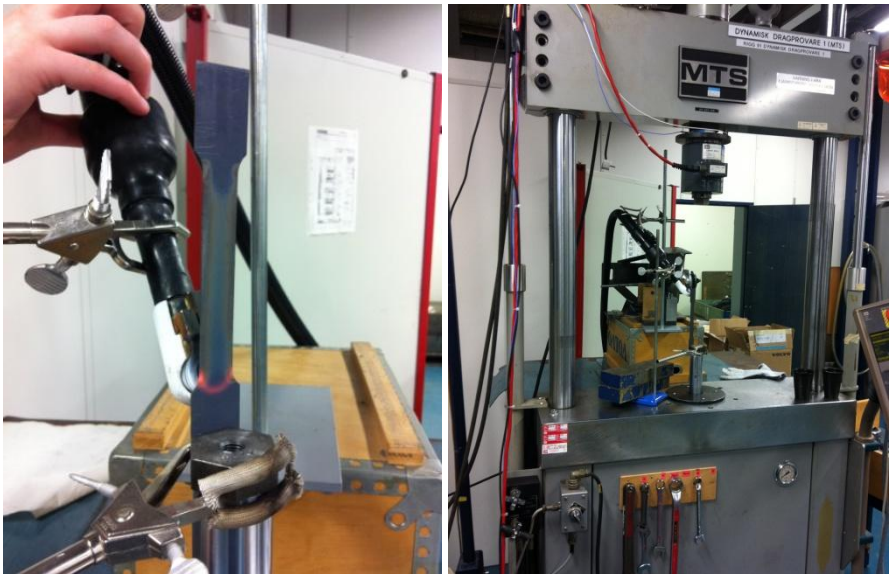

Figure 6: Induction tempering of specimens using a tensile test machine

Ten specimens were tempered at 400°C (4 mm/s), 500°C (3 mm/s) and 600°C (1.8 mm/s) respectively. The input power was not measured during the process. Temperature was measured with a thermo camera of the model Fluke Ti55 to assure the right temperature and to verify an even distribution of the heat. To retrieve the correct emissivity value, the camera was calibrated against the same furnace used during tempering in the first experiment. An emissivity value of 0.8 was used. The camera had a temperature range up to 620°C with an accuracy of 2%. Some issues regarding the thermo camera were observed, see section 7.

Due to the limited temperature range of the thermo camera, specimens were not tempered above 600°C. Instead the test was expanded with specimens tempered at 400°C, to get a broader field of view.

3.4 Tempering of B-pillars

An industrial robot at VCC was used for induction heating of the B-pillars. The induction heater was attached to the robot and moved along the flanges, through a programmed curve, see Figure 7. The B-pillars were taken directly from the production. These were made of uncoated boron steel, not the Al-Si coated Usibor steel used in the earlier experiments. The B-pillars were attached to an existing fixture for welding to increase precision during the heating procedure. Temperature was measured using a thermo camera in the same way as for the specimens. The uncoated boron steel, used in the B-pillars, was covered with an oxide layer during and after tempering. Therefore an emissivity value of 0.9 was used after calibration against the furnace.

The power input was unfortunately unknown, though the speed was strictly controlled to reach the desired temperature of 600°C with an even distribution. Eight B-pillars were tempered using the following process parameters:

- temperature = 600 °C
- length of zones = 400 mm (see Figure 8)
- speed = 2.5-5 mm/sec (along curve)

Figure 7: Induction heating of a B-pillar with an industrial robot programmed to move along the flange.

The B-pillars were tested in a dynamic 3-point drop tower test. B-pillars are simply supported by two beams as an impactor hits a centered point, see Figure 8. The B-pillars were tested with a specific drop tower weight of 77 kg at different velocities. The impactor velocity was varied to find the critical limits for i) fracture in one flange and ii) fracture in both flanges of both the non-tempered (hereafter denoted “fully hardened”) and tempered B-pillars.

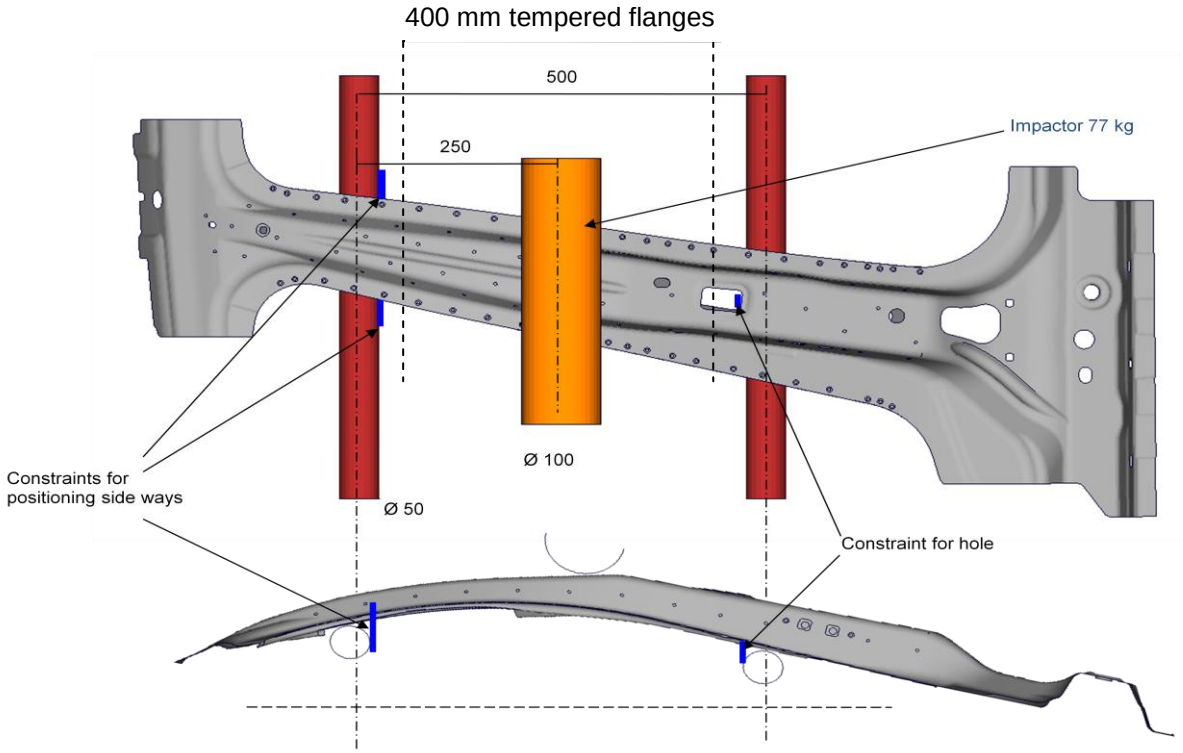

Figure 8: Arrangement for the 3-point drop tower test.

Simulations of dynamic 3-point drop tower test were performed for B-pillars, with help from a CAE engineer at VCC. This was done to get a deeper understanding of the physical 3-point bending test regarding experimental set-up and impactor velocity. The soft zones on the flanges of the B-pillar were modeled with material data for DP600 steel (15).

4 Results

Here follows the results from the experimental series. The non-tempered specimens are also denoted reference.

4.1 Furnace tempering of test specimens

Specimens tempered in a furnace were used for tensile test, hardness test and metallurgical analysis.

4.1.1 Tensile test

For every specimen tested, a standard stress-strain diagram has been created to visualize the results given. For a more specific analysis, detailed lists can be found in Appendix I.

The most important values will be presented here. The primary values and results used and compiled for conclusions are:

- Total elongation at fracture (ε_f)
- Yield strength ($R_{p0.2}$)
- Ultimate tensile strength (R_m)
- Strain hardening ratio ($R_m/R_{p0.2}$)
- Area reduction

The presented diagrams shown below correspond to the "typical" mean value stress-strain diagram given for respective series in the tensile test, i.e. the figures and plots do not show the exact mean values of each series. The plots are manually modified to visualize the results clearer. For more detailed data, Table 4 and Table 5 show the exact mean values for each series at respective temperature. Each series contains a set of five specimens.

Specimens without spot weld

Figure 9 and Table 4 below clearly emphasize the effect of tempering temperature. Since all specimens were tempered for five minutes, it is obvious that the process temperature influences the material properties to a large extent cf. section 2.5. With a gradual increase in temperature, the material hardness and strength decrease, though ductility increases significantly. As seen in Figure 9 and Table 4, the elongation increases from 5% to 11.6 % with increasing temperature at the expense of material yield –and ultimate tensile strength. Also the strain hardening ratio ($R_m/R_{p0.2}$) increases some with the increasing tempering temperature. The strain hardening is however very limited. Noteworthy is that the reference specimens show the highest strain-hardening ratio and fractures significantly earlier than the tempered ones. This parabolic appearance of the reference curve is typical of a strain hardening bcc or bct material. The material starts to plastically deform at 1111 MPa and the stress increases until fracture at 1500 MPa, due to strain hardening.

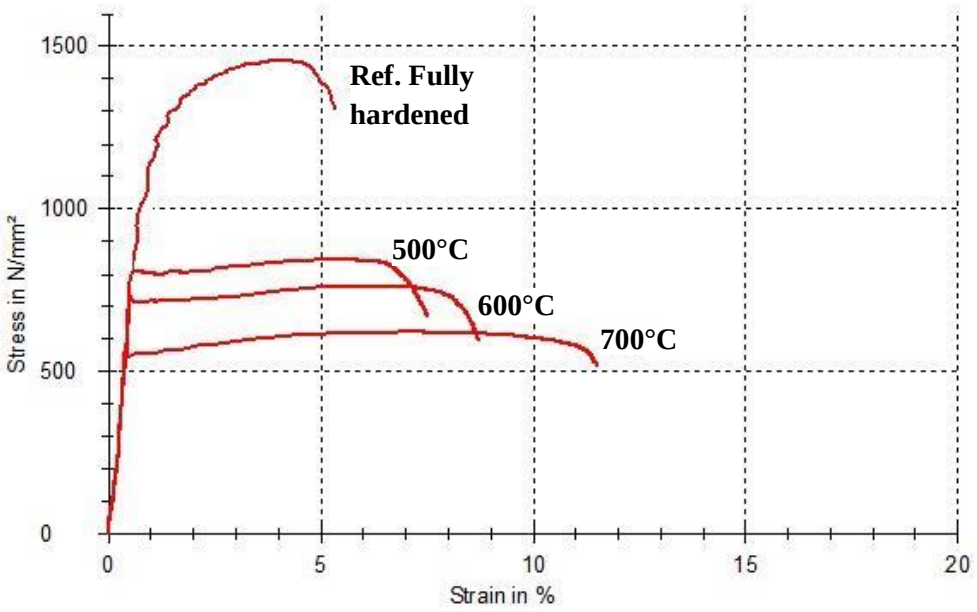

Figure 9: Engineering stress-strain diagram for boron steel specimens tempered in furnace for five minutes at fixed temperatures of 500°C, 600°C and 700°C respectively.

Table 4: Mean values for tensile tests results. Specimens without spot weld tempered furnace.

Temp	ε_f [%]	$R_{p0.2}$ [MPa]	R_m [MPa]	$R_m/R_{p0.2}$ [-]	Hardness [HV1]	Area red. [%]
Ref.	5.0	1111	1500	1.350	463	32
500°C	7.6	821	858	1.045	317	43
600°C	8.8	718	767	1.068	280	47
700°C	11.6	566	633	1.118	220	60

As the material is tempered, it gets softer and weaker as temperature increases, but may withstand a larger elongation. It is important, however, to emphasize the necessary effect of the strain-hardening ratio which reflects the ability of the material to partially deform without a sudden fracture. The material may be exposed to a local high stress, resulting in a local strain and deformation. A material with a high strain-hardening ratio will increase in local strength in this specific area, distributing the strain. However, materials with limited strain-hardening will much certainly develop a local fracture if exposed to high stresses. A material without strain-hardening does not have the ability to increase in strength and to distribute the strain and is therefore very sensitive to local strain.

Somewhat simplified, the appearance of the curve and the value of $R_m/R_{p0.2}$ indicates the capability of the material to withstand stress variations within the structure. All tempered specimens show an almost horizontal curve i.e. exhibits a very limited strain hardening, which indicates a relatively high sensitivity to local stresses.

For specimens tempered at 500°C to 700°C, an increased process temperature results in:

- increase in total elongation (ε_f), i.e. increase in material ductility
- reduction of yield strength, ultimate strength and hardness
- increase in area reduction
- increase in strain-hardening (negligible)

Specimens with spot weld

A spot weld was placed at the center of each specimen, creating a heat affected zone, see Figure 10. A series of five specimens, tempered at each temperature, were tested. Before the test, it was presumed that the tempered specimens with weld would eventually fracture in the HAZ, though with a slight increase in elongation due to the heating process. This was however not the case, since none of the tempered specimens fractured near the spot weld. The negative effect of the HAZ, in terms of short elongation and early crack initiation, was eliminated with the tempering process.

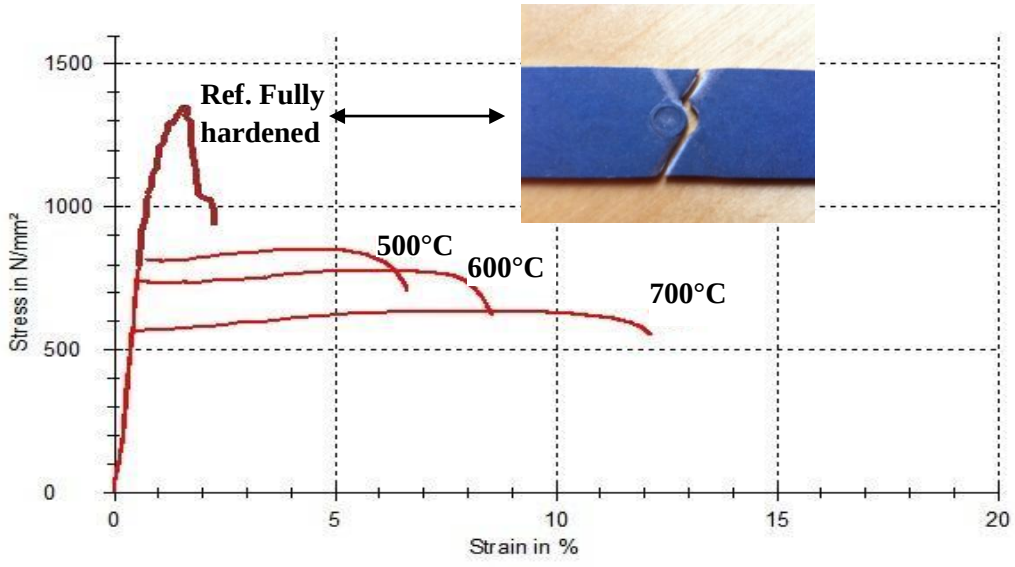

Figure 10: Engineering stress-strain diagram for boron steel specimens tempered in furnace for five minutes at fixed temperatures of 500°C, 600°C and 700°C respectively. Spot weld applied in the middle of the specimen after tempering.

Table 5: Mean values for tensile tests results. Specimens with spot weld tempered in furnace.

Temp	ε_f [%]	$R_{p0.2}$ [MPa]	R_m [MPa]	$R_m/R_{p0.2}$ [-]	Hardness [HV1]	Area red. [%]
Ref.	1.6	1082	1372	1.268	463	28
500°C	6.5	810	848	1.047	317	44
600°C	8.5	723	769	1.064	280	50
700°C	12.3	566	633	1.118	220	60

In comparison to the tempered specimens without spot weld, almost all tempered specimens with weld showed very similar results, concerning fracture strain, hardness and yield- and ultimate strength, see Figure 9 & 10. The tempering treatment has most certainly affected the capability of the material to distribute the deformation in a larger area, eliminating the negative effect of a localized strain in the HAZ. All results associated with the reference specimens decrease as a weld is present. This clearly highlights the fragility of boron steel in HAZ-region, since all welded reference specimens initiate a crack in the HAZ early in the tensile test. The plotted reference curve in Figure 10 clearly shows the effect of crack propagation. The initiation of the crack creates this "shelf-shaped" curve, as remaining material deforms rapidly after crack initiation. The crack then results in fracture and a reduction in both elongation (5% ➔ 1.6 % elongation) and ultimate strength (1500 MPa ➔ 1372 MPa) compared to the reference specimens without weld. A comparison between the fully hardened specimens and the tempered ones can be seen in Figure 11.

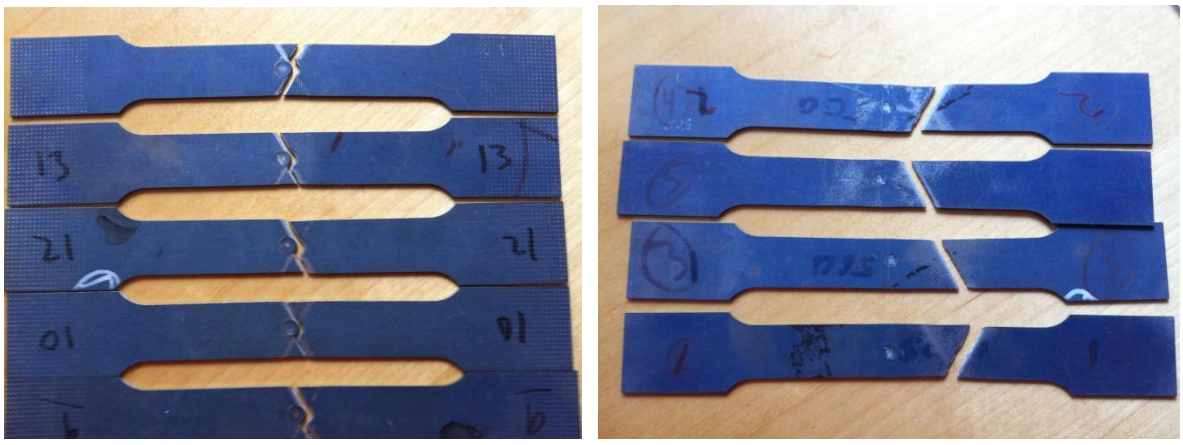

Figure 11: (a) fully tempered specimens show fracture around the spot weld, in HAZ. (b) tempered specimens with spot weld show no fracture in HAZ

As seen in Figure 12, from the ARAMIS measurement, the fracture initiates in the HAZ. This clearly shows the negative effects of HAZ, since the strain is localized to this region, due to difference in strength and hardness within the heat-affected zone and surrounding martensitic material.

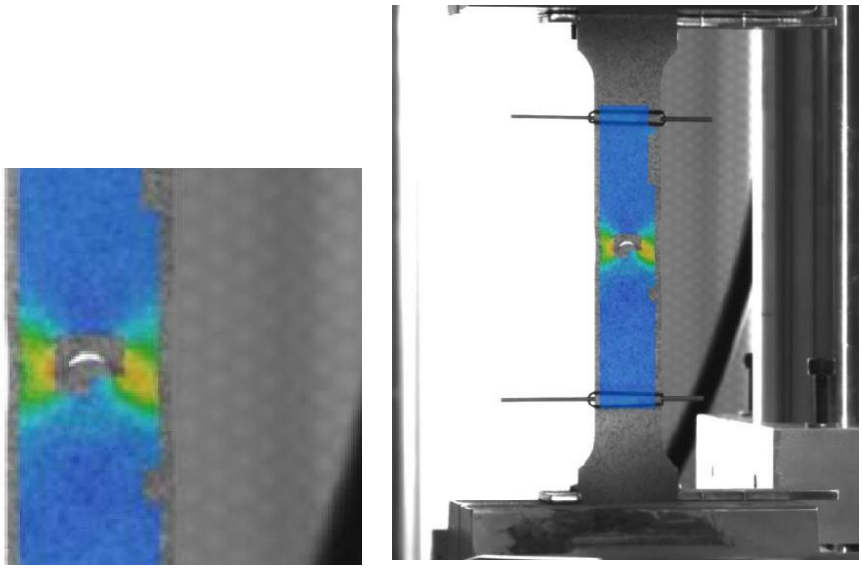

Figure 12: Strain distribution and fracture initiation of a spot welded reference specimen.

Spot weld results in:

Fully hardened specimens (references)

- reduction in total elongation (ε_f), 5 % ➔1.6%
- crack initiation and propagation in HAZ
- reduction of ultimate tensile strength, 1500 MPa ➔ 1372 MPa

Tempered specimens

- negligible change in total elongation(ε_f)
- negligible change of tensile- and ultimate strength
- random placement of crack initiation and fracture

4.1.2 Hardness measurement

The cross-section hardness was similar for all indents on each specimen and the deviation from the mean value did not exceed 10 HV. Indents were made with a distance of 0.4 mm between each measurement. The mean Vickers hardness is shown in Table 4. As expected, the hardness decreases as the tempering temperature increases. The difference in hardness between the untreated reference and the tempered specimens is substantial.

The reduction in hardness and strength in HAZ directs the strain in the welded reference specimens and generated an early fracture. The tempering eliminated the local weak zone that was developed when spot welding in martensitic boron steel. Instead a larger zone is created which has the ability to elongate and distribute strain. This is illustrated in Figure 13.

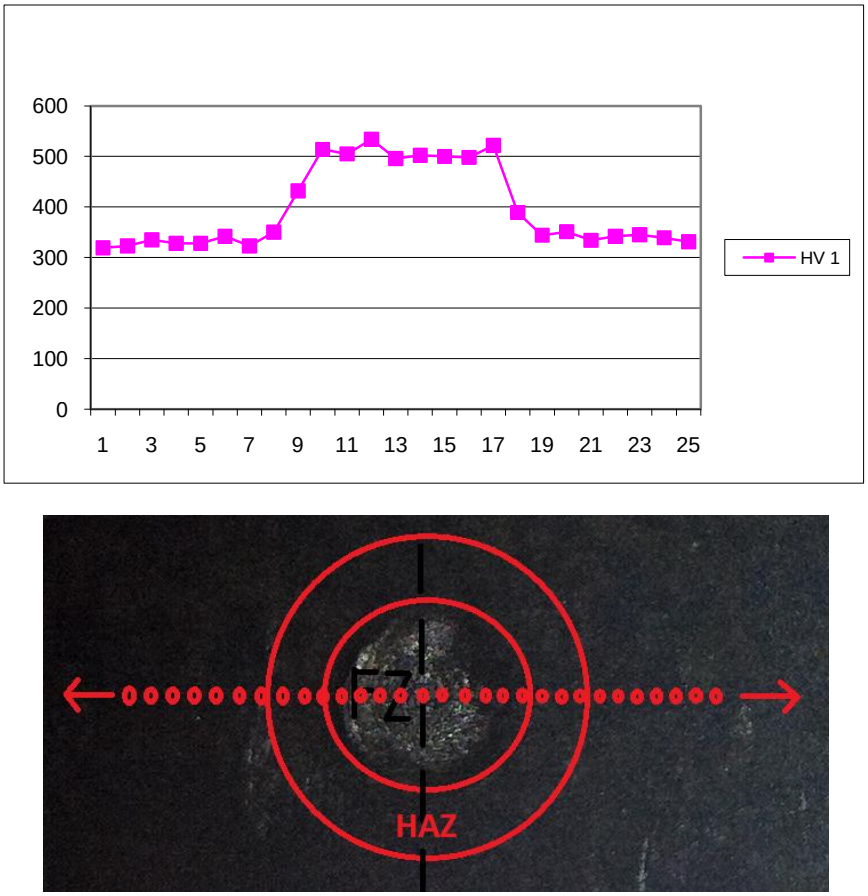

Figure 13: Hardness around spot weld in tempered 22MnB5. Measured over the cross section of a specimen with a weld applied in the middle. The tempering creates a larger soft zone compared to the reference specimen, see Figure 4.

4.1.3 Microstructure and volume change

The results from the metallurgical analysis seen in Figure 14 show the partial structural changes from a typical as-quenched martensite to a fully tempered microstructure. Cementite has started to form carbides in the grain boundaries and within the grains. Tempering becomes more distinct and pronounced as the temperature is increased with larger carbides at the ferrite grain boundaries. This is due to the activation energy (higher heating temperature) that accelerates the transformation to tempered martensite (5). The structural composition is in its initial stage to become a continuous ferrite matrix with a fine dispersion of carbides.

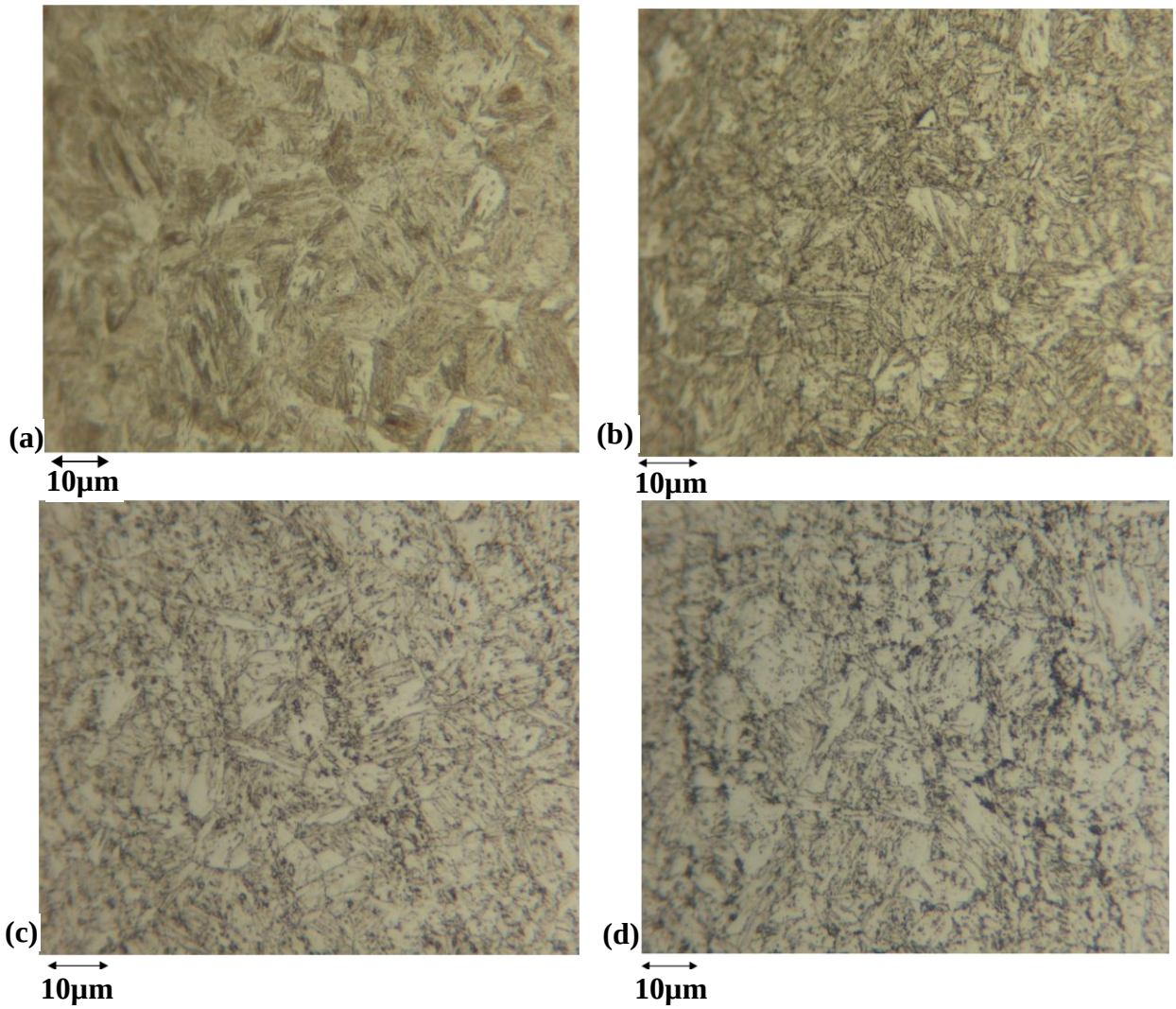

Figure 14: Microstructures for (a) fully hardened 22MnB5 and microstructure after furnace tempering for five minutes at (b) 500°C, (c) 600°C and (d) 700°C. As the temperature increases the carbides in the grain boundaries become more distinct.

The change in length after a tempering process was measured for the temperatures 400°C, 550°C and 700°C. The difference was negligible for all the temperatures, not more than 0.1%.

4.2 Induction tempering of specimens

An identical tensile test series as for the furnace tempering process was carried out for the induction tempered specimens. Here follows the compiled results.

4.2.1 Tensile test

Tensile test were performed in the same way as for the ones tempered in furnace.

Specimens without spot weld

Specimens tempered at 400°C and 500°C showed very poor ductility as compared to specimens tempered in furnace, see Figure 15 and Table 6. All tempered specimens failed outside the extensometer range, see Figure 15. This makes the measured strain arguable since the elongation around the fracture was not measured.

Table 6 clearly emphasizes the increase in area reduction as tempering temperature increases. The value of the area reduction often indicates the capability of the material to deform, i.e. a higher area reduction might show the potential of the material to elongate. These results confirm that the values for of total elongation of the specimens tempered at 400°C and 500°C might be misleading. According to the large area reduction, these specimens should show promising ductility, though this is not the case according to 1.5 % and 2.7% elongation at respective temperature. However, the exact values of the elongation are questionable since issues regarding the measurement with the extensometer did occur. Also, the short elongation may be the effect of a localized strain to the fractured area due to variations in process temperature along the gauge-length, see section 7.

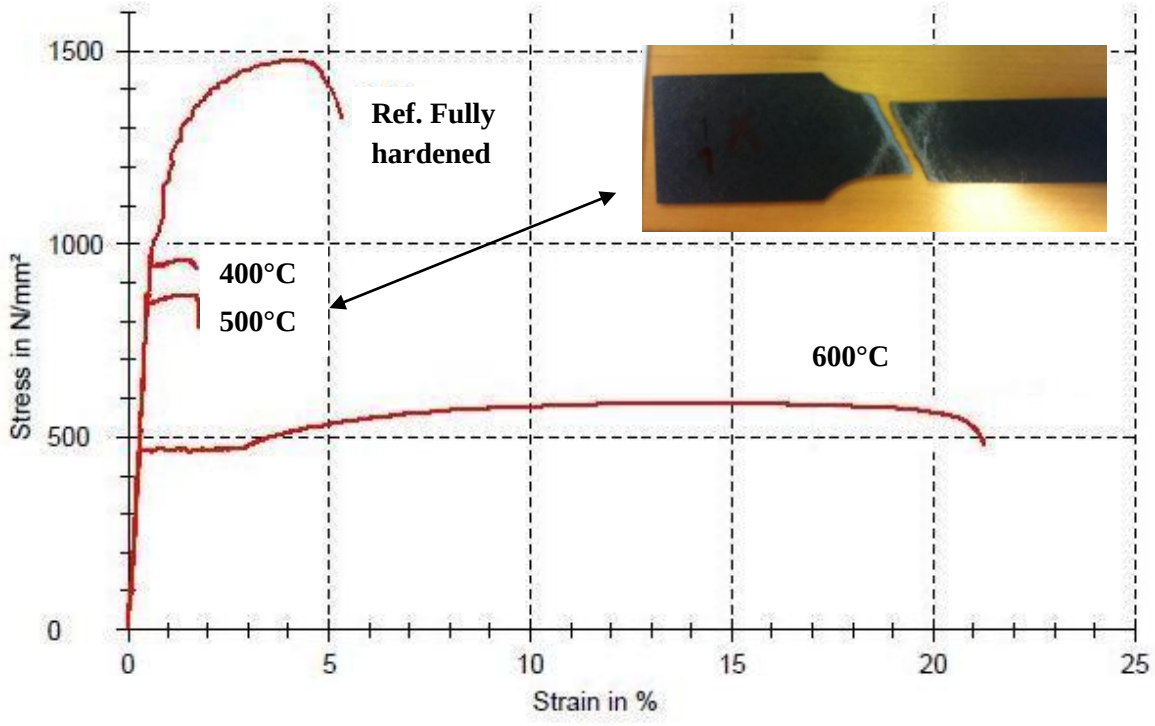

Figure 15: Engineering stress-strain diagram for boron steel specimens tempered using induction heating at temperatures of 400°C, 500°C and 600°C respectively.

Table 6: Mean values for tensile tests results. Specimens without spot weld tempered with induction heating.

Temp	ε_f [%]	$R_{p0.2}$ [MPa]	R_m [MPa]	$R_m/R_{p0.2}$ [-]	Hardness [HV1]	Area red. [%]
Ref.	5	1111	1500	1.350	463	32
400°C	1.5	974	1024	1.051	337	50
500°C	2.7	848	875	1.032	289	56
600°C	21.8	467	592	1.268	196	73

Specimens tempered at 600°C show extreme elongation compared to the earlier results. Also the yield –and ultimate tensile strength and hardness decrease significantly at this specific temperature as compared to references. All specimens induction heat treated at 600°C show similar material properties with a parabolic appearance of the stress-strain curve. This temperature clearly increases the strain-hardening ratio related to other temperatures, which gives the material the ability to elongate substantially more. It is questionable though whether the correct temperature has been achieved, since all material properties imply an even higher temperature than during furnace tempering at 700 °C, see Table 4 & 5. For further analysis and discussion regarding temperature measurement, see section 7.

Induction tempering results in:

- reduction of hardness and yield – and ultimate tensile strength
- decrease in total elongation at 400°C and 500°C
- extreme increase in total elongation at 600°C

Specimens with spot weld

Tempered specimens with a spot weld showed similar material behavior as specimens without a spot weld, see Figure 15 and Figure 16. The same phenomena was observed for specimens tempered in a furnace, see section 4.1. This indicates that the negative effect of the spot weld is eliminated using induction heating. However, it is important to highlight the issues regarding the induction tempering process. As mentioned, for specimens tempered at 400°C and 500°C fracture occurred in the same region. The fracture initiated in the beginning of the waist where the induction heating had started, see Figure 16.

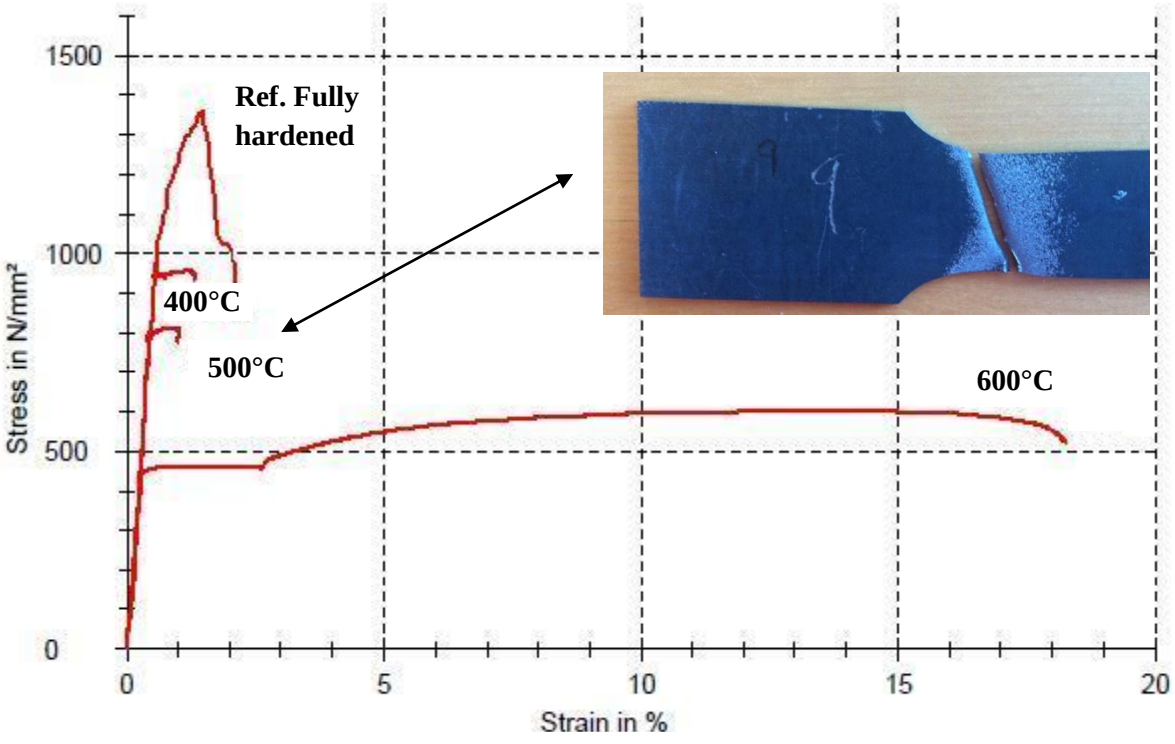

Figure 16: Engineering stress-strain diagram for boron steel specimens tempered using induction heating at temperatures of 400°C, 500°C and 600°C respectively. Spot weld applied in the middle of the specimen after tempering.

Table 7: Mean values for tensile tests results. Induction tempered specimens with a spot weld.

Temp	ε_f [%]	$R_{p0.2}$ [MPa]	R_m [MPa]	$R_m/R_{p0,2}$ [-]	Hardness [HV1]	Area red. [%]
Ref.	1.6	1082	1372	1.268	463	28
400°C	1.1	962	1003	1.043	337	52
500°C	1.3	827	840	1.016	289	58
600°C	18	457	601	1.315	196	70

Induction tempering resulted in:

- reduction of yield strength, ultimate strength and hardness as temperature increases
- decrease in total elongation (ε_f) at 400°C and 500°C
- fracture in the same zone where the induction process started
- extreme increase in total elongation (ε_f) at 600°C

4.2.2 Hardness measurement

The hardness measurement along the gauge-length of a specimen tempered at 500°C indicates that the hardness was significantly lower in the region where fracture occurred, see Figure 17.

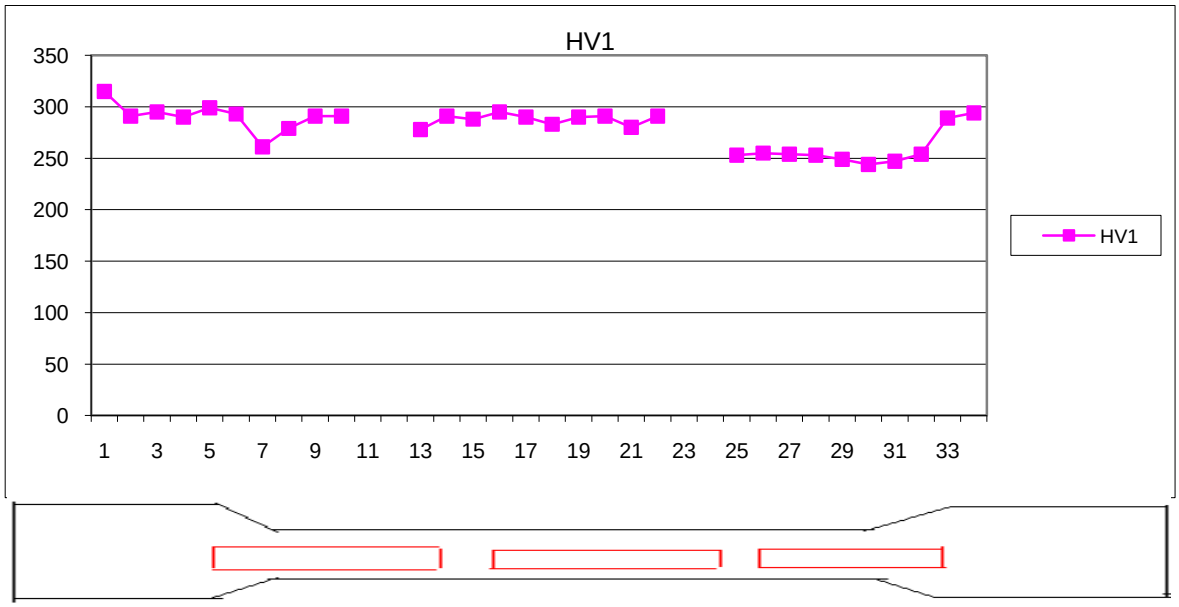

Figure 17: Hardness along specimen, induction tempered at 500°C. The hardness has been measured over the cross sections of the marked areas.

The strain has been localized to this area and the cracking process has been accelerated. Based on these results, it may be concluded that the temperature was not the same along the gauge-length of the specimen, see section 5.

4.3 Induction tempering of B-pillars

Here follows the compiled results from the 3-point drop tower test. For a more specific analysis, detailed lists can be found in Appendix III. Due to secrecy the energy has been normalized, where the lowest energy used in the test corresponds to 1 E.

4.3.1 3-point drop tower test

The primary values and results used and compiled for conclusions and recommendations are:

- dynamic deformation
- crack propagation in flanges

The dynamic deformation of each B-pillar was photographed using a high-speed camera. The photos represent the maximum dynamic deformation during impact with 1.71 E.

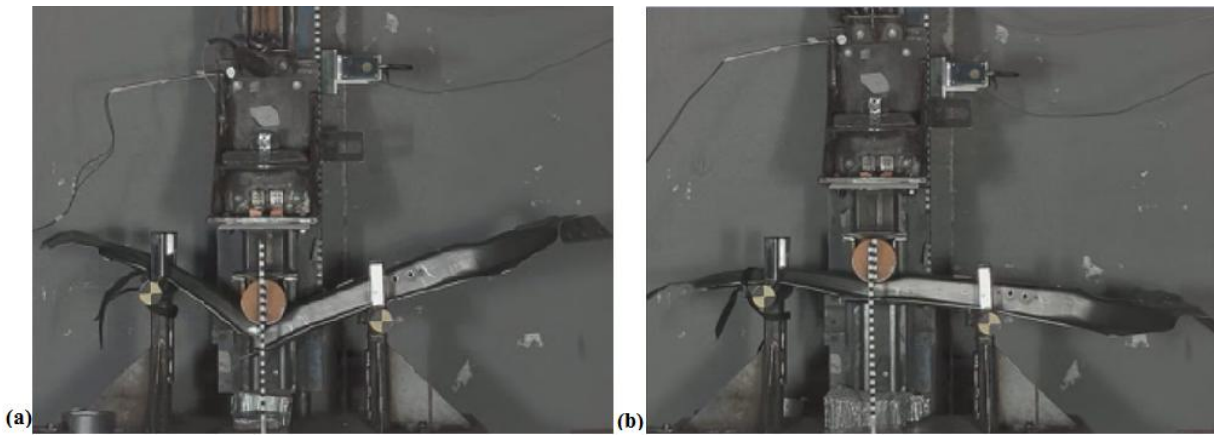

Figure 18: Dynamic deformation at 1.7 E for (a) fully hardened B-pillar and (b) B-pillar with tempered flanges.

Figure 18 clearly shows difference in structural strength of the two B-pillars. It is obvious that the tempered pillar deforms substantially less than the fully hardened at 1.7 E. The soft zones prevent crack propagation in the flanges, increasing strength and reducing deformation. It is important to observe that the fully hardened B-pillar develops two major cracks, reducing strength substantially during impact. This deformation easily accelerates since the pillar offers limited resistance late in the course of impact, due to crack propagation and continuously decreasing strength. The tempered pillars, on the other hand, are only exposed to one major crack at 1.7 E and the structural strength is still sufficiently high to resist an acceleration of the deformation. As told, the difference in strength is relatively high, though it is important to keep in mind that just a slight increase in velocity may be enough for the tempered pillar to develop the same dynamic deformation as the fully hardened.

The values of the dynamic deformation were converted into a plot with respective impact energy for each B-pillar. All B-pillars were divided into the basic categories "Fully hardened"

and "Tempered" and then into sub-categories according to extent of crack initiation, i) no fracture, ii) fracture in one flange and iii) fracture in both flanges.

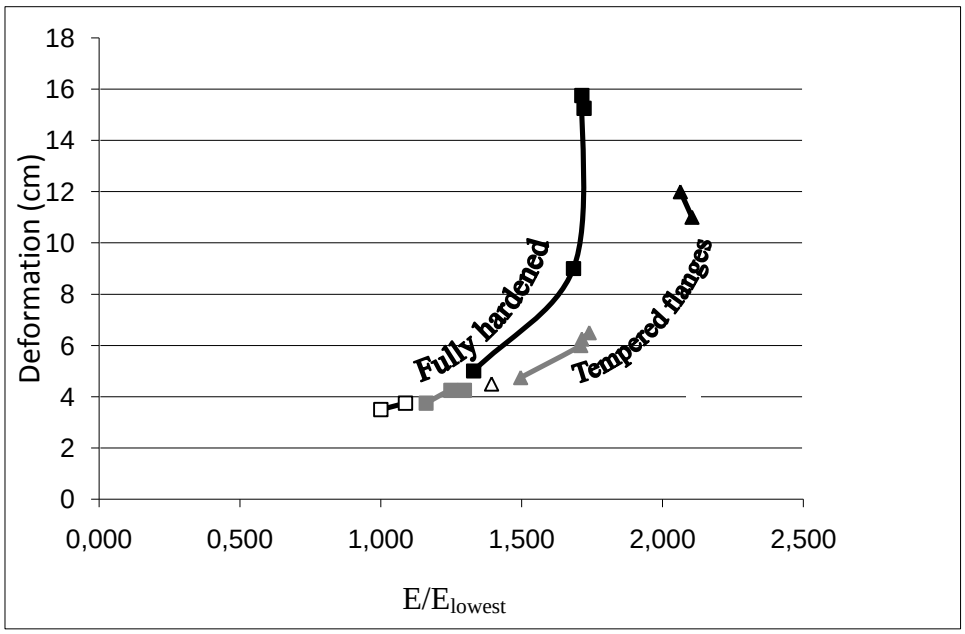

Figure 19: Curves from the 3-point drop tower test showing kinetic energy against the dynamic deformation of the B-pillars. The curves are denoted white) no crack, grey) one crack and black) two cracks.

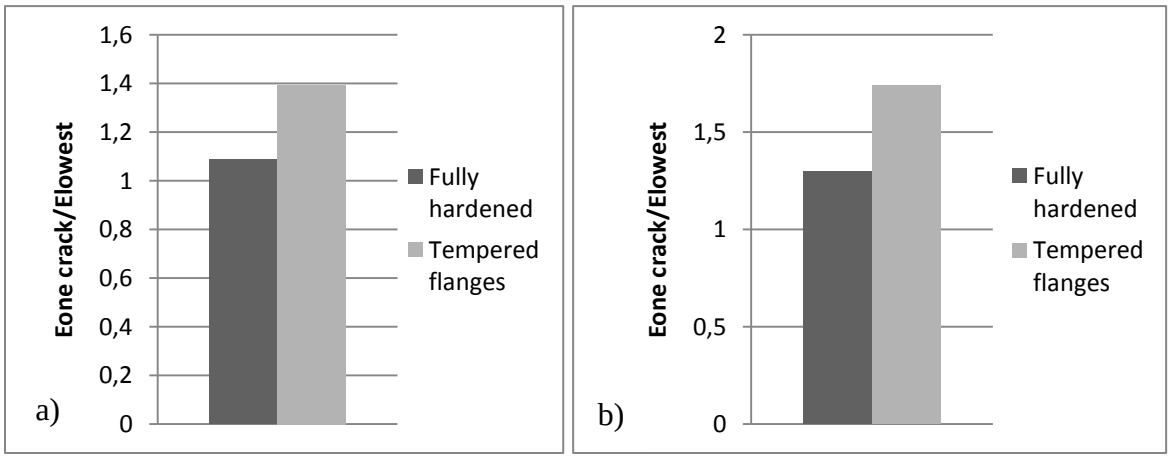

Figure 20: Energy for initiation of (a) crack in one flange, (b) crack in both flanges. The energy has been normalized, where the lowest energy used in the test corresponds to 1 E. At the critical velocity for initiation of two cracks (b), the fully hardened B-pillar withstands 1.3 E and tempered B-pillar 1.74 E. That means the tempered B-pillars are recipient to 30% additional energy compared to fully hardened at the same extent of cracking.

Figure 19 emphasizes the positive effect of a tempering treatment. The B-pillar gets more resistant to cracking, enhancing the structural strength and the ability to absorb kinetic energy. However, as the velocity decreases, the two deformation curves intersect. Tempered B-pillar may have less strength than the reference at lower velocities, as no crack is developed. Noteworthy is also the almost vertical appearance of the fully hardened-curve, which clearly shows the acceleration effect of the deformation as a crack initiate in the structure; a small increase of velocity increases the deformation rapidly. Soft flanges clearly delay this effect. According to Figure 19, the tempered B-pillar is able to absorb substantially more kinetic energy before cracking. At the critical energy for initiation of two cracks, the fully hardened B-pillar withstands 1.3 E with a dynamic deformation of 4.25 cm. At the same level of crack initiation the tempered B-pillar withstands 1.74 E with a dynamic deformation of 6.5 cm. That means the tempered B-pillars are recipient to 30% additional energy compared to fully hardened at the same extent of cracking.

4.3.2 Hardness measurement

The hardness was measured at the tempered flange of a B-pillar, over the cross section around a spot weld, see Figure 21. The figure clearly shows how the small, weak zone around the spot weld has been replaced by a larger zone with a hardness of approximately 260 HV1. According to the furnace tempering that would correspond to a temperature around 650°C.

Figure 21: Hardness measured around a spot weld over the cross section of a flange of a tempered B-pillar. The tempering creates a larger soft zone compared to fully hardened B-pillars.

5 Discussion

Some of the results from the induction tempering of specimens were unexpected, especially for the ones tempered at 600°C. It was discussed whether the camera indicated wrong temperature and if there were some issues linked to the induction process. It was agreed that a hardness of barely 200 HV1 could not be achieved without reaching a higher temperature than 700° as the furnace tempered specimens at that temperature had a hardness of 220 HV1. Therefore, the temperatures indicated in the thermo camera were not likely to be accurate. It is not possible that the temperature have been high enough to form austenite as that would result in a more brittle material upon cooling. However, this temperature shows very promising results considering ductility and strain-hardening why it was implemented as tempering temperature of the B-pillars. It is of great importance to note that this temperature probably is slightly over 700° and not 600°, which was the aim.

All the specimens tempered with induction heating at 400°C and 500°C developed cracks in the zone where the tempering was initiated. Hardness measurement of the specimens showed significantly lower values in this area. The strain has probably been localized to this area leading to an accelerated cracking. Based on these results, it may be concluded that the temperature achieved was not the same along the gauge-length of the specimen.

It might be interesting to more thoroughly investigate and analyze what material properties that are most desirable and beneficial in the flanges i.e. at what temperature tempering should be performed. Should the steel be as ductile as possible or is it desirable to just prevent crack initiation in the heat affected zone? By increasing temperature, the material gets more ductile at the expense of strength. This implies that it is important to not only consider material ductility as the primary objective, since structural strength is the major functionality of the B-pillar. It is however very important to prevent cracking, since the cracks decreases structural strength substantially.

No structured geometrical or tolerance measurement was included in the project, though it is of great interest to investigate the tempering effect on these factors. However, some simple geometrical values were compiled at specific points of the B-pillar for comparison between the fully hardened and the tempered one. These values indicated some geometrical changes after tempering, which should be noticed as an important aspect for further research and development.

6 Conclusions

Short time tempering effects of boron steel using induction heating have been investigated. Different tempering temperatures were carried out using specimens heat treated in furnace and by induction heating. Material properties and effects of spot welds were then analyzed using hardness measurement, metallurgical analysis and tensile test. Based on these results, an appropriate tempering procedure was designed for B-pillar. The structural strength of the B-pillars was then analyzed using a dynamic 3-point drop tower test.

Here are the compiled conclusions from the experiments:

Specimens

- Tempering results in reduced material strength and increased ductility, as compared to reference material – the effects increase as tempering temperature increases.
- Tempering results in reduced strain-hardening ratio, as compared to reference material – the material gets more sensitive to strain localization.
- Tempering temperature has major influence on material properties.
- Reference specimens with spot weld always failed in the HAZ.
- Tempered test specimens with spot weld never failed in the HAZ during tensile testing – the negative effects of the HAZ, in terms of short elongation and early crack initiation, were eliminated with the tempering process.
- The tensile test results of the reference specimens deteriorate when spot welded.
- The tensile test results of the tempered specimens remained unchanged when spot welded.
- Tensile test results show little scatter – the process seems repeatable.
- Temperature measurements should be performed with physical contact - to assure correct temperature reading.

B-pillars

- B-pillars with tempered flanges showed increased resistance to material failure in 3-point drop tower test, as compared to fully hardened B-pillars.
- B-pillars with tempered flanges showed reduced dynamic deformation, as compared to fully hardened B-pillars.
- Tempered B-pillars absorbed approximately 30% additional kinetic energy, as compared to fully hardened B-pillars, at the same extent of crack initiation.
- Fully hardened B-pillars always failed in the HAZ.

7 Recommendations

- Quantify material properties after tempering

  - Since different tempering temperatures create various material properties, it is of great interest to quantify these properties for a wider interval of temperatures. This will most certainly ease the analysis of the tempering temperature effects, since it simplifies a deeper understanding of the tempering process and its effects on material behavior.

- Define desired material properties

  - When increasing temperature, the material gets more ductile at the expense of strength. This implies that it is important to not only consider material ductility as the primary objective, since structural strength is the major functionality of the B-pillar. Therefore it is recommended to investigate and analyze which properties that are the most optimal.

- Find an optimal tempering temperature

  - It is beneficial to investigate which temperature interval that develops the most appropriate material properties. Based on the *quantified material properties* and the *desired material properties*, the most optimal tempering temperature should be determined.

- Find an optimal tempering area for B-pillar

  - It is important to investigate the most optimal way of tempering the B-pillar to maximize the structural strength while reducing treatment time, i.e. avoid time consuming and unnecessary operation and enhance crash performance.

- Measure temperature in an accurate way

  - To assure consistent quality and process precision, it is needed to find a more accurate way of measuring and controlling the temperature. One route could be to measure the temperature through physical contact and thermo elements. The temperature and heat distribution could also be investigated using a CAE-simulation before proceeding to real process.

- Quantify effects on part geometry

  - No structured geometry analysis was included in the study, though some simple measurements were compiled for the fully hardened and tempered B-pillar respectively. These values indicated some consistent geometry changes, which imply that a more thorough geometry analysis is needed as further work.

- Introduce induction tempering in an industrial environment

  - There were obviously some issues measuring the temperature during the induction heating, both with respect to temperature control and temperature distribution. Some problems could be solved by avoiding the movement in the tempering process. Instead,

the heating process should be realized using an inductor that covers the whole tempering zone, which is designed to create a homogenous temperature distribution. As written before, the temperature may be measured by using thermocouples. This would be the most realistic and efficient way of performing induction tempering in an industrial environment. It might require a new design of the inductor for various applications. If using a similar induction process as the one used in this project, it is of great importance to control the movement and position of the induction heater with high precision. The heat generated is very sensitive to the distance between the inductor and the work piece. This may be performed by using a highly sophisticated robot, like the ones used in welding with weld bead tracking. Another route might be to apply a constant pressure between the steel and the induction heater by using a spring.

8 References

1. *Mechanism and modeling of cleavage fracture in simulated Heat-Affected Zone microstructure of a High-Strength Low Alloy Steel.* **A. Lembart-perlade, A.F Gourgues, J.Besson, T. Sturel, A. Pineau.** 2004, METALLURGICAL AND MATERIALS TRANSACTIONS, VOLUME 35, pp. 1039-1053.

2. *Martensitic Structures, Metallography and Microstructures.* **ASM Handbook,.** 2004, ASM Handbook, ASM international, pp. 165-178.

3. *Effect of cooling rate on the high strain rate properties of boron steel.* **A. Bardelcik, C.P. Salisbury, S. Winkler, M.A. Wells, M.J. Worswick.** 2010, International Journal of Impact Engineering 37, pp. 694-702.

4. **Ford Global Technologies.** Engineering material specification. *WSS-M1A322-A3.* s.l. : Ford Global Technologies, 2006.

5. **William D. Callister, Jr.** *Materials science and engineering - an introduction.* New York : John Wiley & Sons, Inc, 2007.

6. *Morphological aspects of martensite–austenite constituents in intercritical and coarse grain heat affected zones of structural steels.* **E. Bonnevie, G. Ferrierea, A. Ikhlefa, D. Kaplanb, J.M. Oraina.** 2004, Material Science and engineering, Volume 285, pp. 352-358.

7. *Exploring Temper Bead.* **Walter J. Sperko, P.E.** 2005, Welding Journal.

8. **ASTM.** *E384: Standard Test Method for Knoop and Vickers Hardness of Materials.* s.l. : ASTM International, 2010.

9. **Bhadeshia, H. K. D. H.** Tempered Martensite, University of Cambridge. [Online] [Cited: May 9, 2011.] http://www.msm.cam.ac.uk/phasetrans/2004/Tempered.Martensite/tempered.martensite.html.

10. **KEY to METALS.** The Tempering of Martensite: Part One. [Online] [Cited: May 9, 2011.] http://www.keytometals.com/Articles/Art127.htm.

11. **Krauss, G.** Microsstructures, Processing, and Properties of Steels. [book auth.] ASM International. *ASM Handbook.* s.l. : ASM International, 1990.

12. *Short-time tempering kinetics of quench hardened pearlitic steels.* **Johan Ahlström, Krste Cvetkovski, Birger Karlsson, Ingo Siller.** Conference proceedings ICTPMCS-2010, 31 May – 2 June 2010, Shanghai, China, 6 pp.

13. *Understanding total elongation*, **Stuart Keeler.** Metalforming Magazine, February, 2007.

14. **Trilion Quality Systems.** Trilion. [Online] 2005. [Cited: May 17, 2011.] http://www.trilion.com/pdf/ARAMIS_RevA_EN.pdf.

15. **Tata Steel Europe**. *Tata Steel Europe.* [Online] [Cited: 2 June 2011.] http://www.tatasteeleurope.com/file_source/StaticFiles/Business_Units/CSPUK/DP600%20Cold%20Datasheet.pdf.

Appendices

I. Tensile tests

II. Hardness tests

III. 3-point drop tower tests

Appendix I -Tensile test results

Fully hardened without a spot weld

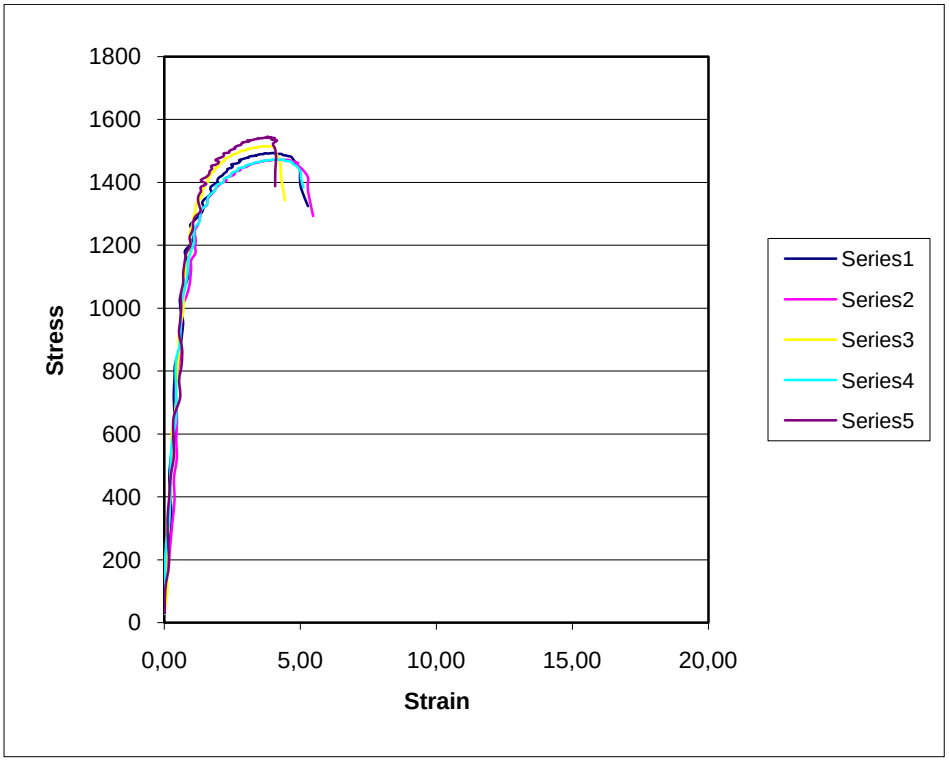

Specimen No.	t [mm]	A80 [%]	Width [mm]	Area [mm^2]	Strain at peak [%]
1	1,23	5,50	19,94	24,53	4,26
2	1,22	5,30	19,92	24,30	4,02
3	1,22	4,50	19,92	24,30	3,71
4	1,22	5,40	19,96	24,35	4,11
5	1,22	4,20	19,95	24,40	3,77
Mean value:	**1,22**	**4,98**	**19,94**	**24,38**	**3,98**

Specimen No.	Rp0,2 [MPa]	Rp2,0 [MPa]	Rm [MPa]
1	1064,40	1392,10	1473,10
2	1113,80	1412,10	1492,50
3	1101,30	1456,60	1515,10
4	1082,60	1393,8	1472,90
5	1193,80	1467,8	1544,50
Mean value:	**1111,18**	**1424,48**	**1499,62**

Fully hardened with a spot weld

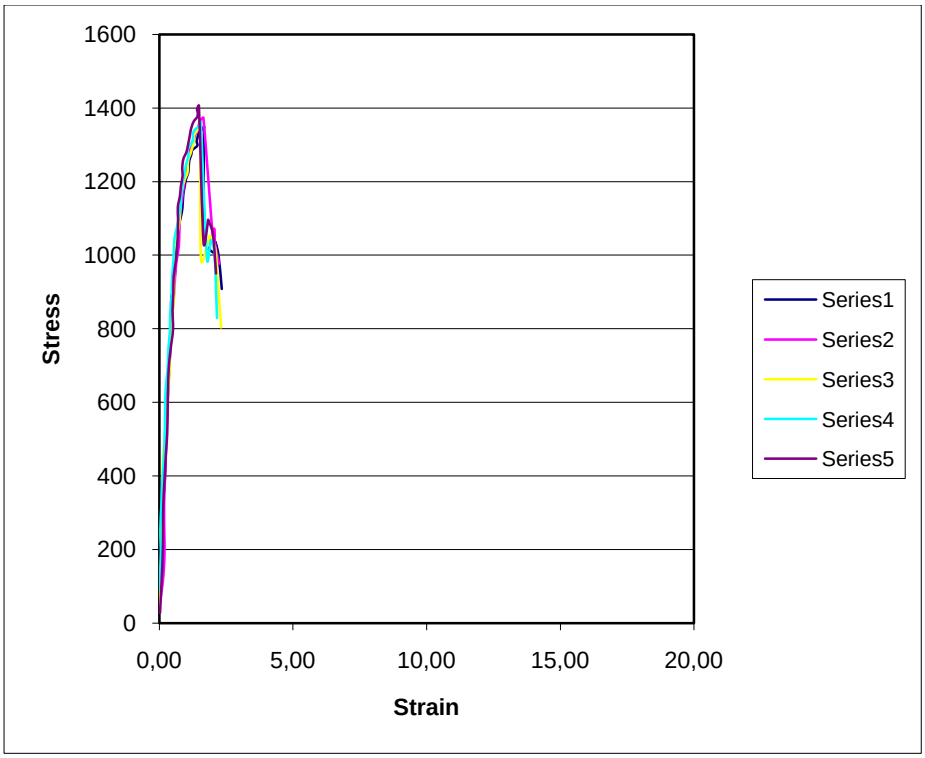

Specimen No.	t [mm]	A80 [%]	Width [mm]	Area [mm^2]	Strain at peak [%]
1	1,22	1,60	19,91	24,29	1,56
2	1,21	1,60	19,92	24,10	1,57
3	1,22	1,50	19,97	24,36	1,54
4	1,23	1,70	20,04	24,65	1,67
5	1,21	1,70	1,92	24,10	1,65
Mean value:	**1,22**	**1,62**	**16,35**	**24,30**	**1,60**

Specimen No.	Rolling dir. [°]	Rp0,2 [MPa]	Rp2,0 [MPa]	Rm [MPa]
1		1096,50	1011,90	1362,40
2		1161,10	1057,50	1409,20
3		1058,20	1034,90	1362,10
4		1082,10	987,90	1355,60
5		1012,30	1029,60	1373,70
Mean value:	-	**1082,04**	**1024,36**	**1372,60**

Zwick / Roell Standard report 08.03.2011

Parameter table:

Material	: 22MNB5
Load cell	: 50 kN
Extensometer	: Longstroke
Machine data	: 50SN3A WN:141202
	Crosshead travel monitor WN:141202
	Load cell ID:0 WN:141203 50 kN
	Longstroke ID:5 WN:141205
Speed Rp, ReH	: 30 N/mm²s
Speed E-Modulus	: 10 mm/min
Pre-load speed	: 10 mm/min
Pre-load	: 20 N

Results:

Nr	Specimen width b0 mm	Specimen thickness a0 mm	EMod kN/mm²	Rp x N/mm²	RB N/mm²	At %	ReH N/mm²	Rm N/mm²
1	19,98	1,23	105,84	841,93	647,59	9,18	842,49	874,32
2	19,93	1,23	140,57	800,46	653,94	7,50	-	843,18
3	19,89	1,23	143,85	812,45	649,19	7,23	-	850,05
4	19,97	1,23	149,61	857,93	686,24	7,34	-	894,24
5	19,93	1,23	140,71	793,63	742,43	6,63	-	829,29

Nr	ε-F max %	εBreak %	Annealing Temp ℃	Weld
1	6,11	9,22	500	No
2	5,31	7,54	500	No
3	4,83	7,28	500	No
4	4,77	7,39	500	No
5	5,05	6,68	500	No

Zwick / Roell Standard report 08.03.201

Series graph:

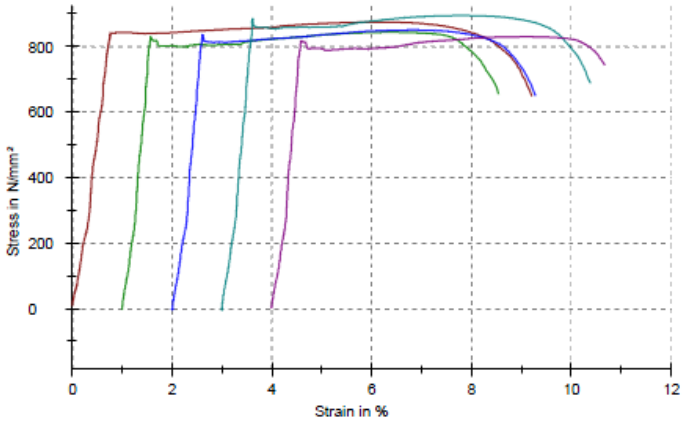

Statistics:

Series n = 5	Specimen width b0 mm	Specimen thickness a0 mm	EMod kN/mm²	Rp x N/mm²	RB N/mm²	At %	ReH N/mm²	Rm N/mm²
$\bar{x}$	19,94	1,23	136,12	821,28	675,88	7,58	842,49	858,22
s	0,03606	0,000	17,32	27,59	40,40	0,95	-	25,92
v	0,18	0,00	12,72	3,36	5,98	12,60	-	3,02

Series n = 5	ε-F max %	εBreak %	Annealing Temp ℃
$\bar{x}$	5,22	7,62	500
s	0,54	0,95	0,000
v	10,39	12,48	0,00

Furnace tempered, 500°C, without a spot weld

Zwick / Roell **Standard report** 09.03.2011

Parameter table:

Material	:	22MNB5
Annealing Temp	:	500 °C
Weld	:	Yes
Load cell	:	50 kN
Extensometer	:	Longstroke
Machine data	:	50SN3A WN:141202
		Crosshead travel monitor WN:141202
		Load cell ID:0 WN:141203 50 kN
		Longstroke ID:5 WN:141205
Speed Rp, ReH	:	30 N/mm²s
Speed E-Modulus	:	10 mm/min
Pre-load speed	:	10 mm/min
Pre-load	:	20 N

Results:

Nr	Specimen width b0 mm	Specimen thickness a0 mm	EMod kN/mm²	Rp x N/mm²	RB N/mm²	At %	ReH N/mm²	Rm N/mm²
1	19,98	1,23	138,76	809,34	674,36	7,30	811,89	847,79
2	19,95	1,23	139,23	810,40	678,63	6,37	-	843,43
3	19,95	1,23	138,13	798,42	632,92	6,12	-	839,08
4	19,95	1,22	140,96	818,90	674,78	6,23	-	858,10
5	19,96	1,22	141,69	814,42	699,68	6,63	815,56	851,72

Nr	ε-F max %	εBreak %
1	5,07	7,34
2	4,29	6,41
3	4,07	6,17
4	4,39	6,28
5	4,58	6,68

Zwick / Roell **Standard report** 09.03.2011

Series graph:

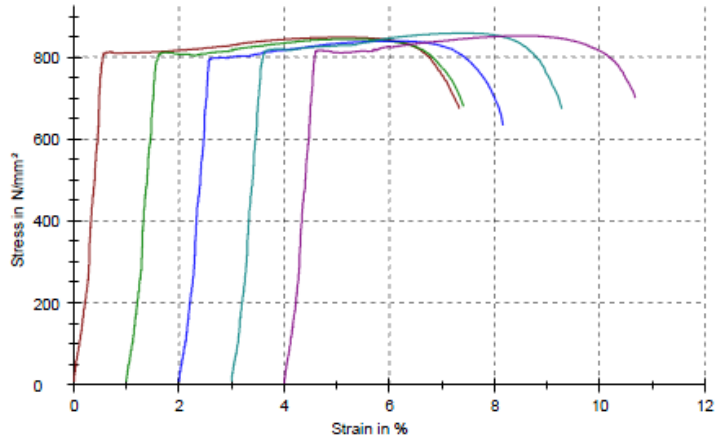

Statistics:

Series n = 5	Specimen width b0 mm	Specimen thickness a0 mm	EMod kN/mm²	Rp x N/mm²	RB N/mm²	At %	ReH N/mm²	Rm N/mm²
x̄	19,96	1,226	139,75	810,30	672,08	6,53	813,73	848,02
s	0,01304	0,005477	1,51	7,63	24,24	0,47	2,60	7,35
v	0,07	0,45	1,08	0,94	3,61	7,20	0,32	0,87

Series n = 5	ε-F max %	εBreak %
x̄	4,48	6,58
s	0,38	0,47
v	8,46	7,09

Furnace tempered, 500°C, with a spot weld

Zwick / Roell **Standard report** 09.03.2011

Parameter table:

Material	:	22MNB5
Annealing Temp	:	600 °C
Weld	:	No
Load cell	:	50 kN
Extensometer	:	Longstroke
Machine data	:	50SN3A WN:141202
		Crosshead travel monitor WN:141202
		Load cell ID:0 WN:141203 50 kN
		Longstroke ID:5 WN:141205
Speed Rp, ReH	:	30 N/mm²s
Speed E-Modulus	:	10 mm/min
Pre-load speed	:	10 mm/min
Pre-load	:	20 N

Results:

Nr	Specimen width b0 mm	Specimen thickness a0 mm	EMod kN/mm²	Rp x N/mm²	RB N/mm²	At %	ReH N/mm²	Rm N/mm²
1	19,97	1,22	123,79	731,47	618,69	8,29	735,21	780,76
2	19,98	1,23	122,47	711,44	581,80	8,73	-	762,06
3	19,96	1,23	119,97	709,23	577,00	7,94	-	760,22
4	19,98	1,23	120,26	713,12	579,42	9,05	-	762,38
5	19,97	1,23	122,19	726,36	618,26	9,75	-	770,57

Nr	ε-F max %	εBreak %
1	6,10	8,32
2	6,21	8,77
3	5,32	7,98
4	5,86	9,08
5	6,02	9,78

Zwick / Roell **Standard report** 09.03.2011

Series graph:

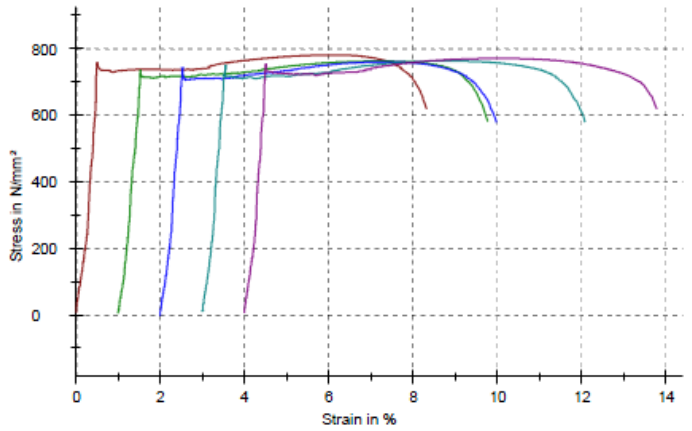

Statistics:

Series n = 5	Specimen width b0 mm	Specimen thickness a0 mm	EMod kN/mm²	Rp x N/mm²	RB N/mm²	At %	ReH N/mm²	Rm N/mm²
$\bar{x}$	19,97	1,228	121,74	718,33	595,03	8,75	735,21	767,20
s	0,008367	0,004472	1,60	9,93	21,46	0,70	-	8,57
v	0,04	0,36	1,32	1,38	3,61	8,02	-	1,12

Series n = 5	ε-F max %	εBreak %
$\bar{x}$	5,90	8,78
s	0,35	0,70
v	5,92	7,95

Furnace tempered, 600°C, without a spot weld

Zwick / Roell **Standard report** 09.03.2011

Parameter table:

Material	:	22MNB5
Annealing Temp	:	600 °C
Weld	:	Yes
Load cell	:	50 kN
Extensometer	:	Longstroke
Machine data	:	50SN3A WN:141202
		Crosshead travel monitor WN:141202
		Load cell ID:0 WN:141203 50 kN
		Longstroke ID:5 WN:141205
Speed Rp, ReH	:	30 N/mm²s
Speed E-Modulus	:	10 mm/min
Pre-load speed	:	10 mm/min
Pre-load	:	20 N

Results:

Nr	Specimen width b0 mm	Specimen thickness a0 mm	EMod kN/mm²	Rp x N/mm²	RB N/mm²	At %	ReH N/mm²	Rm N/mm²
1	19,96	1,23	121,07	714,45	600,88	8,60	714,96	760,66
2	19,96	1,23	120,77	710,39	591,74	8,49	-	759,93
3	19,93	1,22	124,71	733,85	610,19	8,56	-	776,31
4	19,96	1,22	124,75	723,07	596,25	8,61	726,58	770,63
6	19,96	1,21	125,96	736,79	645,47	8,28	737,93	777,78

Nr	ε-F max %	εBreak %
1	5,63	8,64
2	6,05	8,53
3	5,78	8,59
4	5,86	8,65
6	5,70	8,32

Zwick / Roell **Standard report** 09.03.2011

Series graph:

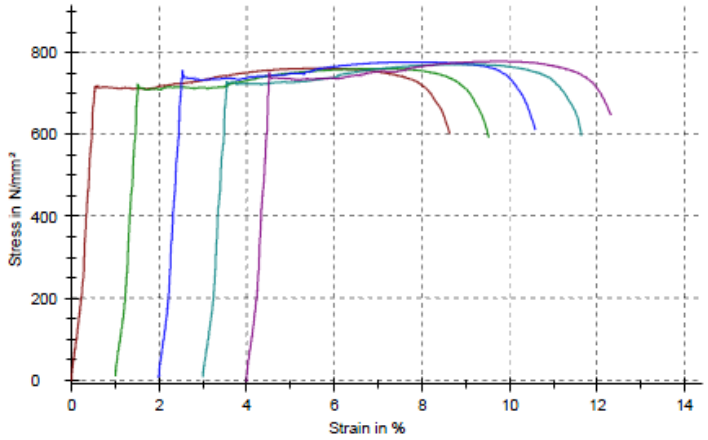

Statistics:

Series n = 5	Specimen width b0 mm	Specimen thickness a0 mm	EMod kN/mm²	Rp x N/mm²	RB N/mm²	At %	ReH N/mm²	Rm N/mm²
$\bar{x}$	19,95	1,222	123,45	723,71	608,91	8,51	726,49	769,06
s	0,01342	0,008367	2,37	11,59	21,55	0,14	11,49	8,44
v	0,07	0,68	1,92	1,60	3,54	1,60	1,58	1,10

Series n = 5	ε-F max %	εBreak %
$\bar{x}$	5,80	8,55
s	0,16	0,14
v	2,83	1,59

Furnace tempered, 600°C, with a spot weld

Zwick / Roell **Standard report** 09.03.2011

Parameter table:

Material	: 22MNB5
Annealing Temp	: 700 °C
Weld	: No
Load cell	: 50 kN
Extensometer	: Longstroke
Machine data	: 50SN3A WN:141202
	Crosshead travel monitor WN:141202
	Load cell ID:0 WN:141203 50 kN
	Longstroke ID:5 WN:141205
Speed Rp, ReH	: 30 N/mm²s
Speed E-Modulus	: 10 mm/min
Pre-load speed	: 10 mm/min
Pre-load	: 20 N

Results:

Nr	Specimen width b0 mm	Specimen thickness a0 mm	EMod kN/mm²	Rp x N/mm²	RB N/mm²	At %	ReH N/mm²	Rm N/mm²
1	19,95	1,2	93,01	583,73	508,21	11,08	-	642,41
2	19,99	1,22	88,89	562,80	505,76	9,40	-	628,50
3	19,96	1,22	86,00	552,95	512,16	11,57	552,64	621,05
4	19,97	1,22	94,28	593,02	541,16	12,72	-	647,94
5	19,94	1,22	82,18	538,98	497,26	13,09	-	625,10

Nr	ε-F max %	εBreak %
1	7,31	11,07
2	5,33	9,39
3	7,20	11,56
4	7,71	12,71
5	8,73	13,07

Zwick / Roell **Standard report** 09.03.2011

Series graph:

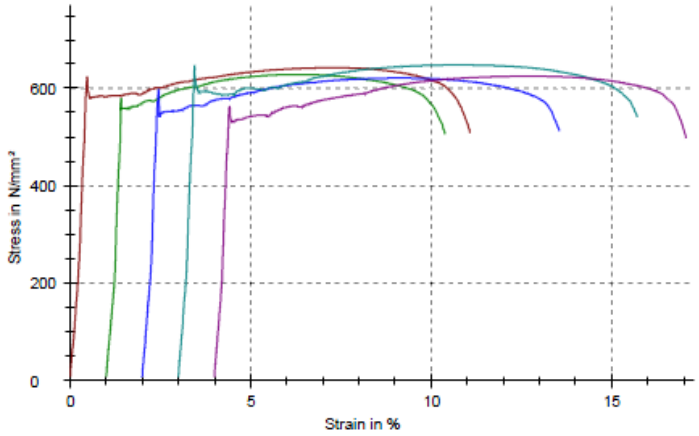

Statistics:

Series n = 5	Specimen width b0 mm	Specimen thickness a0 mm	EMod kN/mm²	Rp x N/mm²	RB N/mm²	At %	ReH N/mm²	Rm N/mm²
x̄	19,96	1,216	88,87	566,30	512,91	11,57	552,64	633,00
s	0,01924	0,008944	4,98	22,10	16,71	1,47	-	11,59
v	0,10	0,74	5,61	3,90	3,26	12,68	-	1,83

Series n = 5	ε-F max %	εBreak %
x̄	7,26	11,56
s	1,23	1,46
v	17,01	12,63

Furnace tempered, 700°C, without a spot weld

Zwick / Roell **Standard report** 09.03.2011

Parameter table:

Material	: 22MNB5
Annealing Temp	: 700 °C
Weld	: Yes
Load cell	: 50 kN
Extensometer	: Longstroke
Machine data	: 50SN3A WN:141202 Crosshead travel monitor WN:141202 Load cell ID:0 WN:141203 50 kN Longstroke ID:5 WN:141205
Speed Rp, ReH	: 30 N/mm²s
Speed E-Modulus	: 10 mm/min
Pre-load speed	: 10 mm/min
Pre-load	: 20 N

Results:

Nr	Specimen width b0 mm	Specimen thickness a0 mm	EMod kN/mm²	Rp x N/mm²	RB N/mm²	At %	ReH N/mm²	Rm N/mm²
1	19,96	1,21	89,73	568,92	490,22	11,48	-	623,40
2	19,91	1,22	84,62	547,01	537,57	13,22	548,01	630,19
3	19,96	1,21	89,42	568,49	540,38	12,20	-	636,02
4	19,96	1,2	86,83	554,88	556,91	14,23	-	640,13
5	19,88	1,21	94,69	593,30	498,80	10,48	-	637,34

Nr	ε-F max %	εBreak %
1	6,74	11,47
2	8,89	13,19
3	8,23	12,19
4	9,02	14,21
5	6,28	10,47

Zwick / Roell **Standard report** 09.03.2011

Series graph:

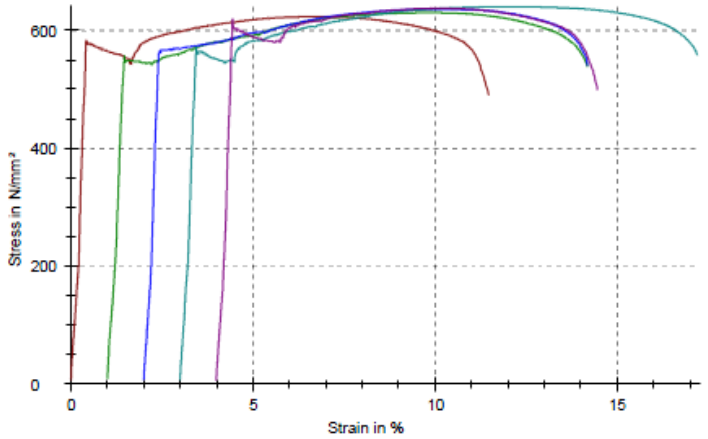

Statistics:

Series n = 5	Specimen width b0 mm	Specimen thickness a0 mm	EMod kN/mm²	Rp x N/mm²	RB N/mm²	At %	ReH N/mm²	Rm N/mm²
x̄	19,93	1,21	89,06	566,52	524,78	12,32	548,01	633,42
s	0,03715	0,007071	3,78	17,63	28,76	1,46	-	6,67
v	0,19	0,58	4,24	3,11	5,48	11,87	-	1,05

Series n = 5	ε-F max %	εBreak %
x̄	7,83	12,31
s	1,26	1,46
v	16,04	11,84

Furnace tempered, 700°C, with a spot weld

Zwick / Roell **Standard report** 07.04.2011

Parameter table:

Material	: 22MNB5
Load cell	: 50 kN
Extensometer	: Longstroke
Machine data	: 50SN3A WN:141202
	Crosshead travel monitor WN:141202
	Load cell ID:0 WN:141203 50 kN
	Longstroke ID:5 WN:141205
Speed Rp, ReH	: 30 N/mm²s
Speed E-Modulus	: 10 mm/min
Pre-load speed	: 10 mm/min
Pre-load	: 20 N

Results:

Nr	Specimen width b0 mm	Specimen thickness a0 mm	EMod kN/mm²	Rp x N/mm²	RB N/mm²	At %	ReH N/mm²	Rm N/mm²
1	19,95	1,22	158,70	943,10	774,44	1,55	945,59	1015,55
2	19,95	1,21	170,94	994,97	772,38	1,11	996,94	1049,32
3	19,93	1,24	160,36	967,72	752,63	1,29	973,46	1019,14
4	19,93	1,25	170,04	982,94	748,37	2,39	989,19	1011,60
5	19,98	1,25	166,10	980,46	752,25	1,12	984,82	1024,24

Nr	ε-F max %	εBreak %	Annealing Temp °C	Weld
1	0,59	1,58	400	No
2	0,60	1,15	400	No
3	0,57	1,31	400	No
4	0,57	2,43	400	No
5	0,58	1,16	400	No

Zwick / Roell **Standard report** 07.04.2011

Series graph:

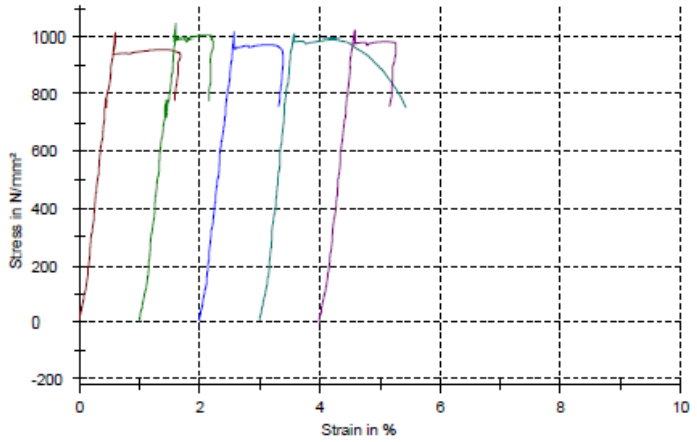

Statistics:

Series n = 5	Specimen width b0 mm	Specimen thickness a0 mm	EMod kN/mm²	Rp x N/mm²	RB N/mm²	At %	ReH N/mm²	Rm N/mm²
x	19,95	1,234	165,23	973,84	760,01	1,49	978,00	1023,97
s	0,02049	0,01817	5,54	19,72	12,36	0,53	20,01	14,91
v	0,10	1,47	3,35	2,02	1,63	35,65	2,05	1,46

Series n = 5	ε-F max %	εBreak %	Annealing Temp °C
x	0,58	1,53	400
s	0,01	0,54	0,000
v	2,28	35,07	0,00

Induction tempered, 400°C, without a spot weld

Zwick / Roell **Standard report** 07.04.2011

Parameter table:

Material	: 22MNB5
Load cell	: 50 kN
Extensometer	: Longstroke
Machine data	: 50SN3A WN:141202
	Crosshead travel monitor WN:141202
	Load cell ID:0 WN:141203 50 kN
	Longstroke ID:5 WN:141205
Speed Rp, ReH	: 30 N/mm²s
Speed E-Modulus	: 10 mm/min
Pre-load speed	: 10 mm/min
Pre-load	: 20 N

Results:

Nr	Specimen width b0 mm	Specimen thickness a0 mm	EMod kN/mm²	Rp x N/mm²	RB N/mm²	At %	ReH N/mm²	Rm N/mm²
1	19,95	1,24	160,68	948,41	759,28	1,16	945,74	998,06
2	19,94	1,25	156,98	926,89	736,08	1,37	927,14	950,68
3	19,94	1,24	167,73	970,87	762,10	1,12	975,68	996,60
4	19,95	1,25	165,62	967,92	751,31	0,95	972,91	1019,68
5	19,96	1,25	170,87	1000,23	829,03	1,18	1008,59	1050,93

Nr	ε-F max %	εBreak %	Annealing Temp ℃	Weld
1	0,58	1,20	400	Yes
2	0,55	1,41	400	Yes
3	0,59	1,16	400	Yes
4	0,61	0,99	400	Yes
5	0,61	1,21	400	Yes

Zwick / Roell **Standard report** 07.04.2011

Series graph:

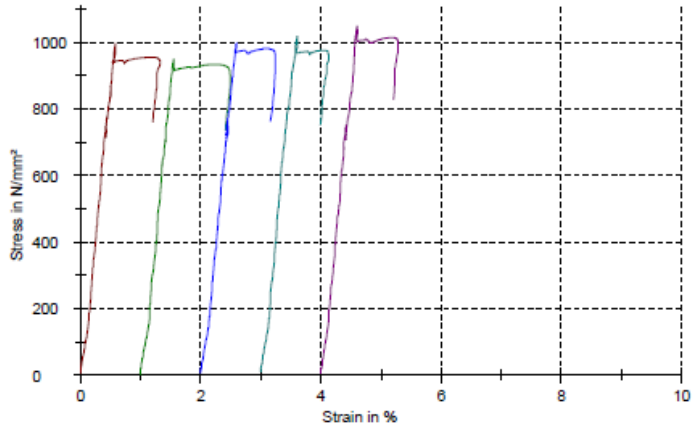

Statistics:

Series n = 5	Specimen width b0 mm	Specimen thickness a0 mm	EMod kN/mm²	Rp x N/mm²	RB N/mm²	At %	ReH N/mm²	Rm N/mm²
x̄	19,95	1,246	164,37	962,86	767,56	1,16	966,01	1003,19
s	0,008367	0,005477	5,55	27,34	35,82	0,15	31,13	36,67
v	0,04	0,44	3,38	2,84	4,67	12,96	3,22	3,65

Series n = 5	ε-F max %	εBreak %	Annealing Temp ℃
x̄	0,59	1,20	400
s	0,02	0,15	0,000
v	3,98	12,48	0,00

Induction tempered, 400°C, with a spot weld

Zwick / Roell Standard report 07.04.2011

Parameter table:

Material	: 22MNB5
Load cell	: 50 kN
Extensometer	: Longstroke
Machine data	: 50SN3A WN:141202
	Crosshead travel monitor WN:141202
	Load cell ID:0 WN:141203 50 kN
	Longstroke ID:5 WN:141205
Speed Rp, ReH	: 30 N/mm²s
Speed E-Modulus	: 10 mm/min
Pre-load speed	: 10 mm/min
Pre-load	: 20 N

Results:

Nr	Specimen width b0 mm	Specimen thickness a0 mm	EMod kN/mm²	Rp x N/mm²	RB N/mm²	At %	ReH N/mm²	Rm N/mm²
1	19,96	1,22	126,96	864,78	732,61	1,79	-	891,11
2	19,98	1,23	140,06	851,86	707,56	1,57	-	888,34
3	19,98	1,23	126,50	826,18	713,69	4,63	-	847,38
4	19,96	1,23	-	-	664,46	-	-	768,13
5	19,94	1,24	-	-	682,60	-	-	782,20

Nr	ε-F max %	εBreak %	Annealing Temp °C	Weld
1	0,47	1,74	500	No
2	0,53	1,59	500	No
3	0,44	4,61	500	No
4	0,41	0,39	500	No
5	0,50	0,49	500	No

Zwick / Roell Standard report 07.04.2011

Series graph:

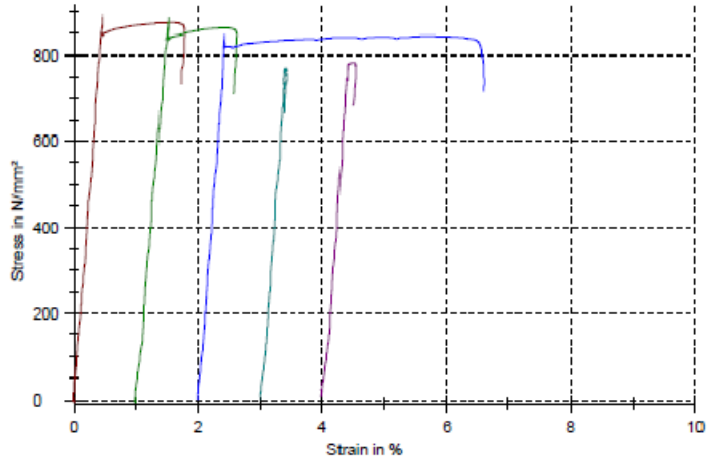

Statistics:

Series n = 5	Specimen width b0 mm	Specimen thickness a0 mm	EMod kN/mm²	Rp x N/mm²	RB N/mm²	At %	ReH N/mm²	Rm N/mm²
x̄	19,96	1,23	131,17	847,61	700,18	2,66	-	835,43
s	0,01673	0,007071	7,70	19,65	26,80	1,71	-	57,89
v	0,08	0,57	5,87	2,32	3,83	64,08	-	6,93

Series n = 5	ε-F max %	εBreak %	Annealing Temp °C
x̄	0,47	1,76	500
s	0,05	1,70	0,000
v	10,54	96,62	0,00

Induction tempered, 500°C, without a spot weld

Zwick / Roell Standard report 07.04.2011

Parameter table:

Material	: 22MNB5
Load cell	: 50 kN
Extensometer	: Longstroke
Machine data	: 50SN3A WN:141202
	Crosshead travel monitor WN:141202
	Load cell ID:0 WN:141203 50 kN
	Longstroke ID:5 WN:141205
Speed Rp, ReH	: 30 N/mm²s
Speed E-Modulus	: 10 mm/min
Pre-load speed	: 10 mm/min
Pre-load	: 20 N

Results:

Nr	Specimen width b0 mm	Specimen thickness a0 mm	EMod kN/mm²	Rp x N/mm²	RB N/mm²	At %	ReH N/mm²	Rm N/mm²
1	19,93	1,23	135,43	842,39	676,95	2,55	-	869,32
2	19,9	1,24	122,22	811,16	667,33	0,98	-	812,74
3	19,97	1,24	108,82	-	665,07	0,78	762,89	762,89
4	19,93	1,25	117,10	-	627,06	0,66	757,62	757,62

Nr	ε-F max %	εBreak %	Annealing Temp °C	Weld
1	0,49	2,56	500	Yes
2	0,94	0,95	500	Yes
3	0,63	0,71	500	Yes
4	0,67	0,64	500	Yes

Series graph:

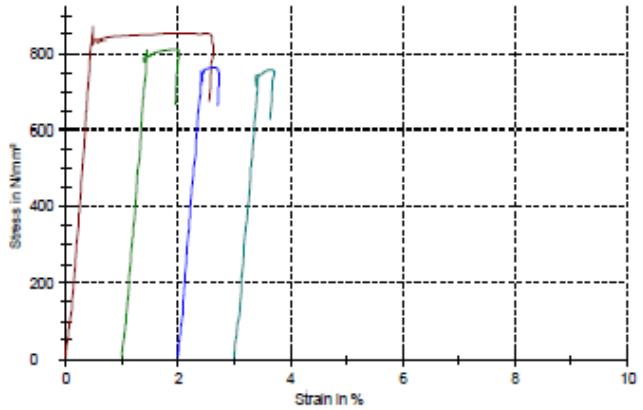

Zwick / Roell Standard report 07.04.2011

Statistics:

Series n = 4	Specimen width b0 mm	Specimen thickness a0 mm	EMod kN/mm²	Rp x N/mm²	RB N/mm²	At %	ReH N/mm²	Rm N/mm²
x̄	19,93	1,24	120,89	826,77	659,11	1,24	760,26	800,64
s	0,02872	0,008165	11,15	22,06	21,97	0,88	3,72	52,09
v	0,14	0,66	9,22	2,67	3,33	70,79	0,49	6,51

Series n = 4	ε-F max %	εBreak %	Annealing Temp °C
x̄	0,68	1,21	500
s	0,19	0,91	0,000
v	27,57	74,71	0,00

Induction tempered, 500°C, with a spot weld

Zwick / Roell **Standard report** 07.04.2011

Parameter table:

Material	: 22MNB5
Load cell	: 50 kN
Extensometer	: Longstroke
Machine data	: 50SN3A WN:141202
	Crosshead travel monitor WN:141202
	Load cell ID:0 WN:141203 50 kN
	Longstroke ID:5 WN:141205
Speed Rp, ReH	: 30 N/mm²s
Speed E-Modulus	: 10 mm/min
Pre-load speed	: 10 mm/min
Pre-load	: 20 N

Results:

Nr	Specimen width b0 mm	Specimen thickness a0 mm	EMod kN/mm²	Rp x N/mm²	RB N/mm²	At %	ReH N/mm²	Rm N/mm²
1	19,93	1,24	56,00	460,57	471,73	23,52	-	597,11
2	19,93	1,24	98,22	635,06	540,42	15,34	-	681,87
3	19,98	1,24	67,25	472,28	522,69	17,63	476,02	596,53
4	19,95	1,25	65,18	470,28	447,05	24,20	-	588,86
5	19,99	1,23	97,82	631,23	550,14	13,88	633,11	690,43

Nr	ε-F max %	εBreak %	Annealing Temp ℃	Weld
1	14,95	23,32	600	No
2	0,40	15,32	600	No
3	12,97	17,55	600	No
4	15,17	24,11	600	No
5	0,41	13,86	600	No

Zwick / Roell **Standard report** 07.04.2011

Series graph:

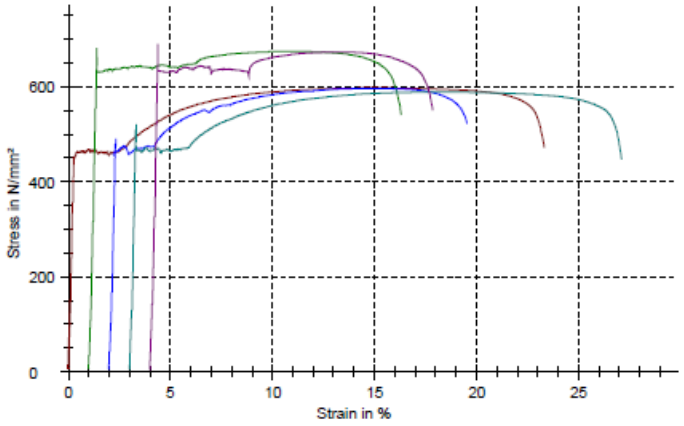

Statistics:

Series n = 5	Specimen width b0 mm	Specimen thickness a0 mm	EMod kN/mm²	Rp x N/mm²	RB N/mm²	At %	ReH N/mm²	Rm N/mm²
x̄	19,96	1,24	76,90	533,88	506,40	18,91	554,57	630,96
s	0,02793	0,007071	19,75	90,73	44,89	4,72	111,08	50,58
v	0,14	0,57	25,68	16,99	8,86	24,93	20,03	8,02

Series n = 5	ε-F max %	εBreak %	Annealing Temp ℃
x̄	8,78	18,83	600
s	7,69	4,66	0,000
v	87,64	24,73	0,00

Induction tempered, 600°C, without a spot weld

Zwick / Roell Standard report 07.04.2011

Parameter table:

Material	: 22MNB5
Load cell	: 50 kN
Extensometer	: Longstroke
Machine data	: 50SN3A WN:141202
	Crosshead travel monitor WN:141202
	Load cell ID:0 WN:141203 50 kN
	Longstroke ID:5 WN:141205
Speed Rp, ReH	: 30 N/mm²s
Speed E-Modulus	: 10 mm/min
Pre-load speed	: 10 mm/min
Pre-load	: 20 N

Results:

Nr	Specimen width b0 mm	Specimen thickness a0 mm	EMod kN/mm²	Rp x N/mm²	RB N/mm²	At %	ReH N/mm²	Rm N/mm²
1	19,96	1,23	60,30	460,49	509,45	18,47	-	602,39
2	19,96	1,25	56,13	444,92	513,06	16,34	-	591,27
3	19,96	1,23	97,21	535,98	556,74	14,78	-	672,15
4	19,78	1,23	62,88	468,67	492,34	18,86	470,16	606,55

Nr	εF max %	εBreak %	Annealing Temp °C	Weld
1	13,62	18,34	600	Yes
2	11,82	16,19	600	Yes
3	9,80	14,75	600	Yes
4	13,62	18,74	600	Yes

Series graph:

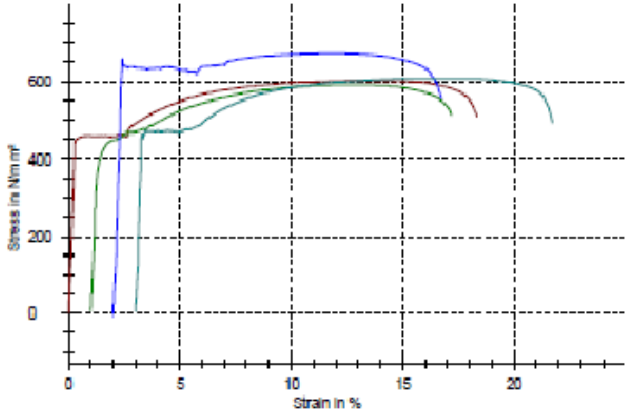

Zwick / Roell Standard report 07.04.2011

Statistics:

Series n = 4	Specimen width b0 mm	Specimen thickness a0 mm	EMod kN/mm²	Rp x N/mm²	RB N/mm²	At %	ReH N/mm²	Rm N/mm²
x̄	19,91	1,235	69,13	502,51	517,90	17,11	470,16	618,59
s	0,085	0,01	18,92	89,52	27,43	1,91	-	36,42
v	0,43	0,81	27,37	17,81	5,30	11,17	-	5,89

Series n = 4	εF max %	εBreak %	Annealing Temp °C
x̄	12,26	17,00	600
s	1,87	1,87	0,000
v	15,27	11,01	0,00

Induction tempered, 600°C, with a spot weld

Appendix II Hardness test

HV1		*Furnace tempering*			*Induction tempering*		
	Ref.	**500°C**	**600°C**	**700°C**	**400°C**	**500°C**	**600°C**
	456	323	278	226	343	291	199
	453	310	284	216	331	290	192
	472	312	267	213	332	283	198
	475	315	281	223	346	290	199
	464	322	284	221	332	291	197
	458	318	281	217	338	288	189
Average	**463**	**317**	**280**	**220**	**337**	**289**	**196**

Appendix III 3-point drop tower test B-Pillar

No.	E(Standardized)	Dynamic def.(cm)	Crack right flange	Crack left flange	Crack patch right	Crack patch left	Crack inforcement right	Crack inforcement left
Fully hardened								
12	1	3,5						
13	1,088	3,75						
11	1,160	3,75	x				x	
14	1,248	4,25	x				x	
16	1,297	4,25	x		x		x	
10	1,330	5	x	x	x		x	x
2	1,684	9	x	x	x	x	x	x
7	1,714	15,75	x	x	x	x	x	x
3	1,721	15,25	x	x	x	x	x	x
Tempered								
17	1,393	4,5						
15	1,496	4,75	x				x	
4	1,710	6	x				x	x
6	1,714	6,25	x		x		x	x
18	1,740	6,5	x		x		x	x
9	2,063	12	x	x	x	x	x	x
8	2,104	11	x	x	x	x	x	x